https://doi.org/10.5194/nhess-2023-33
Preprint. Discussion started: 28 February 2023

Natural Hazards and Earth System Sciences
Discussions
Open Access
EGU

COMPREHENSIVE LANDSLIDE SUSCEPTIBILITY MAP OF CENTRAL ASIA

Ascanio Rosi[a,b], William Frodella[b,c,*], Nicola Nocentini[b,c], Francesco Caleca[b,c], Hans Balder Havenith[d], Alexander Strom[e,f], Veronica Tofani [b,c]

[a] Department of Geosciences, University of Padua, Via G. Gradenigo 6, 35131, Padua, Italy

[b] UNESCO Chair on the Prevention and Sustainable Management of Geo-Hydrological Hazards, University of Florence, Largo Fermi 2, 50125 Florence, Italy

[c] University of Florence, Department of Earth Sciences, via G. la Pira 4, 50121 Florence, Italy.

[d] Department of Geology, University of Liege, 4000 Liege, Belgium

[e] Geodynamics Research Center LLC, Moscow, 125008, Russian Federation

[f] Geodynamics Research Center - branch of JSC "Hydroproject Institute", Moscow, 125993, Russian Federation

* Correspondence: william.frodella@unifi.it; +39 055 2755979

Abstract

Central Asia is an area characterized by complex tectonics and active deformation; the related seismic activity controls the earthquake hazard level that, due to the occurrence of secondary and tertiary effects, has also direct implications on the hazard related to mass movements as landslides, which are responsible for an extensive number of casualties every year. Climatically, this region is characterized by strong rainfall gradient contrasts, due to the diversity of climate and vegetation zones. The region is drained by large, partly snow- and glacier-fed rivers, that cross or terminate in arid forelands; therefore, it is affected also by a significant river flood hazard, mainly in spring and summer seasons. The challenge posed by the combination of different hazards can only be tackled considering a multi-hazard approach harmonized among the different countries, in agreement with the requirements of the Sendai Framework for Disaster Risk Reduction. This work was carried out within the framework of the SFRARR Project ("*Strengthening Financial Resilience and Accelerating Risk Reduction in Central Asia*") as a part of a multi-hazard approach, and is focused on the first landslide susceptibility analysis at a regional scale for Central Asia. To this aim the most detailed landslide inventories, covering both national and transboundary territories were implemented in a Random Forest model, together with several independent variables. The proposed approach represents an innovation in terms of resolution (from 30 to 70 m) and extension of the analysed area with respect to previous regional landslide susceptibility and hazard zonation models applied in Central Asia. The final aim was to provide a useful tool for land use-planning and risk reduction strategies to landslide scientists, practitioners and administrators.

1. Introduction

During the two decades spanning between 1988 and 2007, according to observed estimates, out of 177 reported disasters in Central Asia 13% were landslides, causing 700 deaths (Table 1), while in the same period economic losses have been as high as $150 million, including damage to infrastructures, settlings and agricultural/pasture

https://doi.org/10.5194/nhess-2023-33
Preprint. Discussion started: 28 February 2023

Natural Hazards and Earth System Sciences
Discussions

lands, as well as displacement of the population (GFDRR, 2009). More recent modelled estimates show that in the Central Asia states an annual average of 3 million persons are affected by earthquakes and floods, with an estimated annual average GDP of 9 billion USD (GFDRR, 2016).

Table 1: Observed landslide hazard statistics (1988-2007). Source: Risk assessment for Central Asia and Caucasus (UN ISDR, 2009).

Country	No. disasters/year	Total no. of deaths	Deaths/year	Relative vulnerability (deaths/year/million)
Kazakhstan	0.05	48	2.40	0.16
Kyrgyz Republic	0.30	238	11.90	2.27
Tajikistan	0.50	339	16.95	2.51
Turkmenistan	n.a.	n.a.	n.a.	n.a.
Uzbekistan	0.15	75	3.75	0.14

Due to their large size and impact, most of the occurring landslides have profound transboundary implications. Tajikistan and Kyrgyz Republic are the countries most impacted by landslides: in Tajikistan around 50000 landslide were mapped, 1,200 of which threaten settlements or facilities (Thurman, 2011), while Kyrgyz Republic has been affected by 5,000 landslides, of which 3,500 at various levels of activity are located in the southern portion of the country (the Fergana Valley area) (Pusch, 2004; Li et al., 2021). Only in Kyrgyz Republic, up to 2017, 784 landslides and 1658 mudflows (also including loess flows) and flash floods caused 352 victims (Kalmetieva et al., 2009; Havenith et al., 2015a; 2017). Almaty province in Kazakhstan, Tashkent, Samarkand, Surkhandarya, Kashkadarya Provinces of Uzbekistan, and Ahal Province of Turkmenistan are also exposed to landslides (World Bank, 2006). Given the increased anthropogenic pressures and the impact of climate change, since the early '90s several projects have tried to improve the knowledge on landslide hazard (Thurman, 2011), by providing landslide losses estimations, location, type, triggering/reactivation dates, inventories and hazard/risk maps, as well as platforms to retrieve open disaster risk data and overviews on landslide risk reduction strategies. Amongst the regional studies on landslide hazard, providing descriptions, statistics, and inventory maps, it is worth mentioning:

- Disaster Risk Management and Climate Change Adaptation in Europe and Central Asia, developed by the World Bank - Global Facility for Disaster Reduction and Recovery (Pollner et al., 2010).
- Disaster Risk Reduction, 20 Examples of Good Practice from Central Asia, developed by the European Union, International Strategy for Disaster Reduction ISDR (European Commission Humanitarian Aid, Civil Protection, 2006).
- Science for Peace Project (983289) 'Prevention of landslide dam disasters in the Tien Shan, LADATSHA'. 2009–2012, NATO Emerging Security Challenges Division.

https://doi.org/10.5194/nhess-2023-33
Preprint. Discussion started: 28 February 2023

Natural Hazards and Earth System Sciences
Discussions

- PROGRESS (Potsdam Research Cluster for Georisk Analysis, Environmental Change and Sustainability). German Federal Ministry of Research and Technology (BMBF).
- Tian Shan-Pamir Monitoring Program (TIPTIMON). German Federal Ministry of Education and Research (BMBF).
- M126 IPL Project (funded by the International Consortium on Landslides): M2002111 Detailed study of the internal structure of large rockslide dams in the Tien Shan; M2004126 Compilation of landslide/rockslide inventory of the Tien Shan Mountain System.

Besides the creation of landslide inventories, a common approach to assess landslide hazard is the development of landslide susceptibility maps (LSMs), which depict the relative probability of occurrence of a given type of landslide in a given area, without considering the probability of occurrence in time (Brabb, 1984). In other words, LSMs identify those areas where landslides can occur, based on their geological, morphological, and climatic characteristics. These maps have been extensively used as useful tools for land planning (Cascini 2008; Frattini et al., 2010) and hazard assessment (Corominas et al., 2003). More recently, they have been successfully integrated also in quantitative risk assessment (Chen et al., 2016), and early warning systems (Segoni et al., 2018: Tiranti et al., 2019). LSMs have been produced by applying a wide range of mathematical techniques, from the most traditional statistic approaches like frequency ratio (Yilmaz, 2009), discriminant analysis (Carrara, 1983; Trigila et al., 2013) and logistic regression (Lee, 2005; Duman et al., 2006; Manzo et al., 2013), to more recent and more advanced techniques, like artificial neural network (Tien Bui et al., 2016; Ermini et al., 2005), machine learning (Catani et al., 2013) and multi criteria decision analysis (Akgun, 2012). Statistical-probabilistic models for landslide susceptibility can overcome the data gaps and allow to analyse very wide areas (from basin to national scales), by adopting a homogeneous methodology and a harmonized dataset (including global and local data sources). However, landslide hazard assessment is a complex process since it needs accurate knowledge of the topic and appropriate input data (historical inventories, and regional inventories that consist of large prehistoric events mainly). In this work the landslide susceptibility analysis was carried out by means of the "Random Forest" machine learning algorithm, which is credited as one of the most advanced and reliable techniques in this field (Catani et al., 2013, Goetz et al 2015). This work represents the first landslide susceptibility analysis at a regional scale for Central Asia, and was carried out in the framework of the SFRARR Project ("Strengthening Financial Resilience and Accelerating Risk Reduction in Central Asia") as a part of a multi-hazard approach (Bazzurro et al., in prep). The main challenge of this work was the creation of a unique LSM of the whole Central Asia, that involved the use of a wide range of variables, to account the features of each country, a high volume of input data, and the development of new approaches to analyse these data and to take into accounts possible discrepancies and non-homogeneities. The proposed approach represents an innovation in terms of resolution, extension of the analysed area with respect to previous regional landslide susceptibility and hazard zonation models applied in Central Asia (e.g., Nadim et al., 2006; Havenith et al., 2015b; Stanley and Kirshbaum, 2017; Pittore et al., 2018; World Bank, 2020). For the studied area the landslide susceptibility distribution in the area covered by elements at risk, such as roads, railways, and buildings, was also assessed (Scaini et al., in prep).

https://doi.org/10.5194/nhess-2023-33
Preprint. Discussion started: 28 February 2023

Natural Hazards and Earth System Sciences
Discussions
Open Access
EGU

2. Study area

Geographically, Central Asia is a vast and diverse region including high mountain chains, deserts, and steppes (Fig. 1). A large portion of the Central Asia countries, especially the southern and eastern parts of the region, are occupied by the mountainous areas of the Djungaria, Tien Shan, Pamir, Kopetdag, and small part of Western Altaj, with peaks above 7,000 m a.s.l (Strom, 2010). These intraplate mountain systems formed in the Cenozoic between the Tarim Basin and the Kazakh Shield, as a result of the India-Asian collision (Molnar and Tapponier 1975, Abdrakhmatov et al., 1996; 2003; Zubovich et al., 2010, Ullah et al., 2015). This work is focused in the most inner part of Central Asia, represented by the territories of Turkmenistan, Kazakhstan, Kyrgyz Republic, Uzbekistan, and Tajikistan. Active mountain building started in the Oligocene (Chedia 1980) or even later (Abdrakhmatov et al. 1996), forming a complex system of basement folds disrupted by numerous thrusts and reverse faults with significant amount of lateral offset (Delvaux et al. 2001). Several regional fault zones are aligned along large parts of the mountain belts, others cross the orogen in a NW-SE direction, e.g., the Talas-Fergana fault, which forms a distinct boundary between the western and central Tien Shan (Trifonov et al. 1992) (Fig. 2).

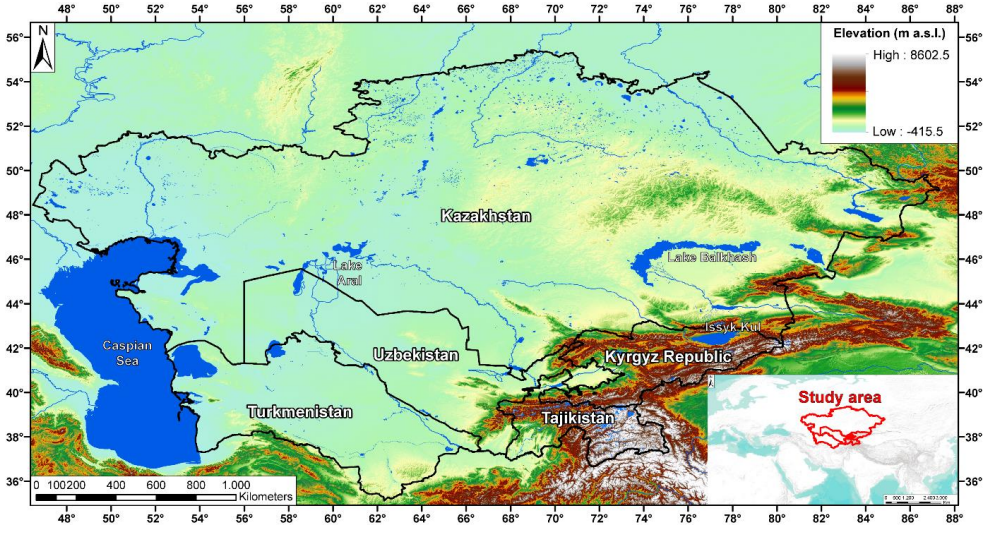

Figure 1. **Study area geographical-geomorphological setting.** Lakes' polygons from Schiavina et al., 2022, while MERIT DEM (Yamazaki et al. 2017) was used as topographic base.

Mountain ridges, formed mainly by palaeozoic crystalline rocks, are separated by wide lenticular or narrow, linear intermountain depressions, containing Neogene and Quaternary deposits, mainly sandstone, siltstone with gypsum interbeds, and conglomerates (Strom and Abdrakhmatov, 2017). Mesozoic and Paleogene deposits are typical of the foothill areas. Almost every ridge, especially in the Tien Shan, corresponds to a neotectonic anticline, and most of the main river valleys follow intermontane tectonic depressions, which are linked by narrow deep gorges up to 1-2 km deep (Strom and Abdrakhmatov, 2018). These mountain systems are the sources of most of Central Asia rivers, which, being fed by glaciers, snowmelt water and rain, have deeply incised valleys.

https://doi.org/10.5194/nhess-2023-33
Preprint. Discussion started: 28 February 2023

Natural Hazards and Earth System Sciences
Discussions
Open Access
EGU

Such extreme topography along with complex geological structure, active tectonics and high seismicity determine important landslide predisposing factors, making landslides the third most prevalent natural hazard in Central Asia, following earthquakes and floods (CAC DRMI, 2009; Havenit et al, 2017).

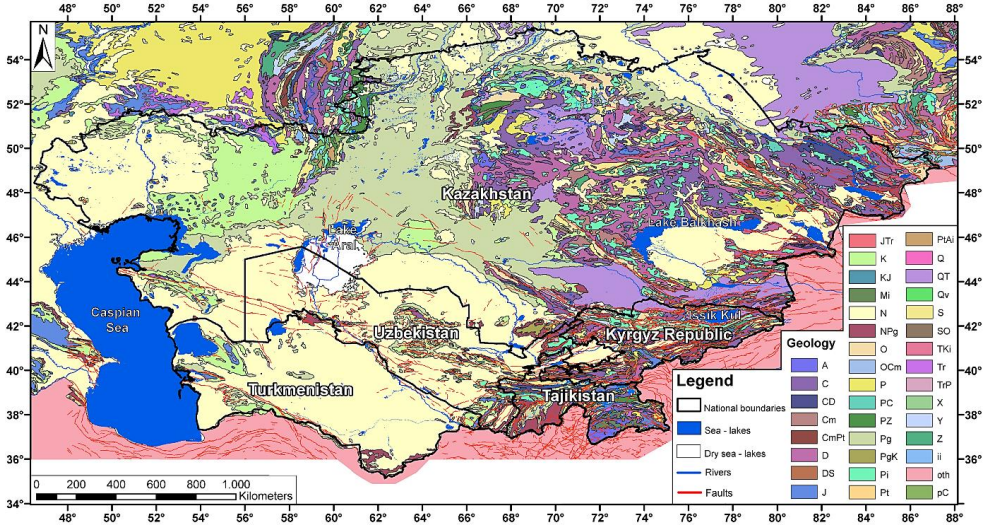

Figure 2. Geological map of the study area. Geological formation data from United States Geological Survey (see Persits et al., 1997 for the legend), including faults from the AFEAD (Active Faults of Eurasia) database (Styron and Pagani, 2020).

2.1 Landslide types in Central Asia

According to the international Cruden and Varnes 1996 classification, landslides phenomena in Central Asia include rockslides/rock avalanches, rotational/translational slides and mud/debris flows (often involving loess), which are triggered by natural events such as earthquakes, floods, rainfall and snowmelt (Behling et al., 2014; 2016; Golovko, 2015; Havenith et al., 2006a,b, 2015a, b; Kalmetieva et al., 2009; Saponaro et al., 2014; 2015; Strom and Abdrakhmatov, 2017; 2018). Glacial lakes outburst flood phenomena, caused by the breech of natural glacial dams, often result in large scale catastrophic mud/debris flows. In Central Asia, landslides more often occur in the loess zone of contact with other rocks, on clay interlayers of the Mesozoic and Cenozoic age, reaching a volume from tens of thousands up to 15-40 $*10^6 m^3$ (Juliev et al., 2017). Seismically triggered landslides are very common in tectonically active mountain regions, such as Tien Shan and Pamir (Sternberg et al., 2006; Hong et al., 2007; Juliev et al., 2017). According to the literature background, most of the large mapped mass movements (especially those with a volume of more than 10^6 m^3) were triggered generally by major (also prehistoric) earthquakes, possibly in combination with climatic factors, namely snowmelt and heavy rainfall (Havenith et al., 2003; Strom and Korup, 2006; Strom, 2010; Schlögel et al., 2011; Strom and Abdrakhmatov 2017, 2018; Havenith et al., 2015a; 2016; Behling et al., 2014; 2016; Piroton et al., 2020). Furthermore, in the past few decades, the number and intensity of landslides have grown owing to climate change and the increase of the anthropic pressure, due to several factors such as the uncontrolled land and water use, the rising of the water tables (often induced by

https://doi.org/10.5194/nhess-2023-33
Preprint. Discussion started: 28 February 2023

Natural Hazards and Earth System Sciences
Discussions

the increase of irrigation; Ishihara et al., 1990), mining, and excavation activities (Pollner et al., 2010; Thurman, 2011).

2.2 Large Rockslides and natural dams

Numerous rockslides have occurred in the mountains producing hazardous natural phenomena such as long runout rock avalanches (Fig. 3) and dammed lakes, more than 100 of which still store water (Strom, 2010). These mainly involve the Palaeozoic magmatic and metamorphic crystalline bedrock, but also the sandstone and limestone formations. Although according to Strom, 2010, many of the existing dammed lakes should be considered as stable, catastrophic outburst floods that occurred in the 20th century, emphasize high potential hazard of landslide natural blockages. Havenith et al., 2015a report a catalogue of large to giant landslides (having volumes exceeding >10^7 m^3) in the Tien Shan area, showing several information such as location, time of occurrence, volumes, and thickness. Regarding the volumes of these rockslides, these range from 50*10^3 m^3 to 10 km^3 (Strom and Korup, 2006; Strom and Abdrakhmatov, 2018). Many of these phenomena, though not all, were triggered by earthquakes with M > 6 and have dammed a river valley (some of the dams have been naturally or artificially breached)

Figure 3. Examples of large rockslide features in Central Asia. Helicopter view of the Usoi landslide scarp, triggered by the 1911 earthquake, Tajikistan (a) (after Strom, 2010); Khait rock avalanche (b) (after Havenith et al., 2015a); helicopter view of Ananevo landslides (c) (after Havenith et al., 2015a).

2.3. Landslide in soft rocks and loose deposits

Rotational landslides mostly occur in loose unconsolidated Quaternary deposits, and in soft and semi-hard rock layers in Mesozoic-Cenozoic sediments, represented mainly by layers of clays, claystones, siltstones, sandstones, marls, limestone, gypsum, and conglomerates, with intercalated clays (Roessner et al., 2004; Kalmetieva et al., 2009) (Fig. 4). These phenomena can create river dams, but they rarely are long-living dams, since usually they are small and their bodies are eroded quickly even if they block a river channel (Strom and Korup, 2006). The loess landslides occur quite regularly (on a yearly basis) in the regions presenting an almost continuous and locally

https://doi.org/10.5194/nhess-2023-33
Preprint. Discussion started: 28 February 2023

Natural Hazards and Earth System Sciences
Discussions

very thick (>20 m) cover of this material, generally at mid-mountain altitude (900 - 2,300 m) and mainly along the border of the Fergana Basin (Kyrgyz Republic, Uzbekistan, and Tajikistan), and on the southern border of the Tien Shan in Tajikistan (Fig. 4).

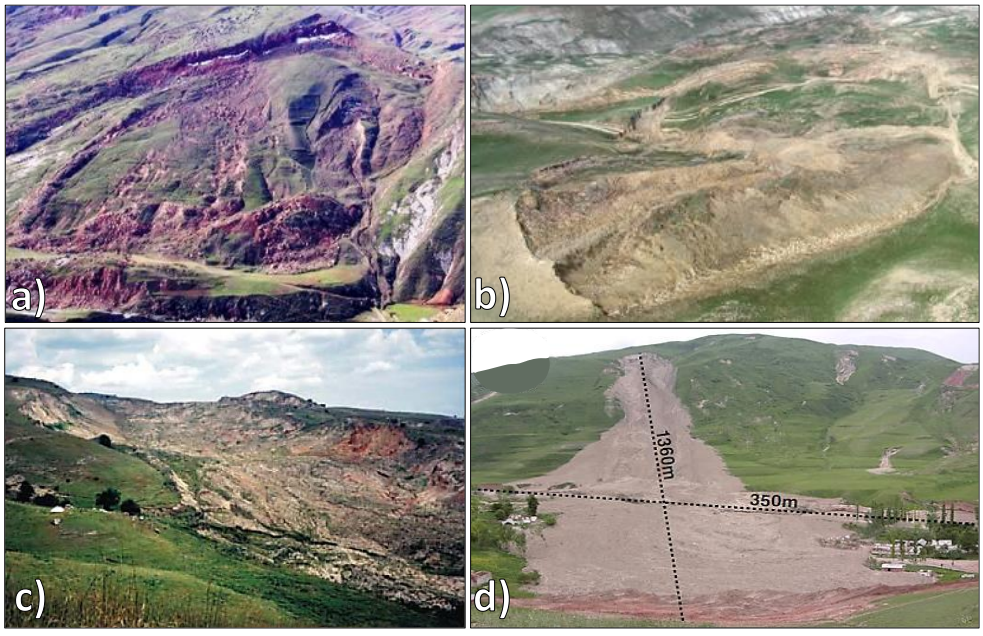

Figure 4. Examples of landslides in soft rocks-loose deposits. Picture the Kamar landslide (a) and the Beshbulak landslide (b) (after Niyazov and Nurtaev, 2013). Examples of loess slides and mixed loess—soft landslides in NE Fergana valley: Kochkor-Ata landslide failure in spring 1994 (c) (after Roessner et al., 2005); Field photo of the Kainama landslide (d) (after Behling et al., 2016).

Loess flow landslides and debris flows, involving the eluvial slope cover, represent a relevant hazardous phenomenon in the mountainous regions of Kazakhstan, in the area of Almaty, near the southern border with Kyrgyz Republic, in the Altai area (Medeu and Blagovechshenskiy, 2016), around the Fergana Basin, all along the border between Tajikistan and Kyrgyz Republic and around the Tajik Depression. Landslides occurring in Quaternary loess units of up to 50 meters thick are characterized by very rapid avalanche-like mass movements, which can reach several meters per second (often represent a combination of rotational slide and dry flow resulting in long runout zones; World Bank, 2008). Typically, pure loess landslides have a volume of hundreds up to one million cubic meters and appear as clusters (Roessner et al., 2005). From the recent history it appears that pure (or quasi-pure) loess slides and flows are particularly dangerous because of their high velocity and long runout which, in turn, can generate a great destructive power and more severe disasters than other types of mass movements of similar size (Havenith et al., 2015a; Behling et al., 2014; 2016). If failure also affects underlying materials (mostly Mesozoic and Cenozoic soft rocks), the volume of these mixed slides can exceed 10×10^6 m^3. These kinds of landslides are particularly deadly and can be triggered by a combination of long-term slope destabilization factors (e.g., rainfall and snowmelt) and short-term triggers (e.g., seismic shocks).

https://doi.org/10.5194/nhess-2023-33
Preprint. Discussion started: 28 February 2023

Natural Hazards and Earth System Sciences
Discussions

Even though earthquake-triggered loess slides and flows are far less frequent than rainfall triggered ones, they caused much larger disasters in recent history, such as those triggered, respectively, by the July 1949 Khait and the January 1989 Gissar earthquakes. The number of active debris flow basins in Kazakhstan is over 300 with registered cases of more than 600 debris flows of different genesis (80% of which are represented by heavy rainfall-triggered debris flows, while the glacial debris flows make up about 15% of the total) (Yaning, C., 1992).

3 Materials and Methods

3.1 Landslide databases

To implement the adopted susceptibility models the largest, most accurate, and updated landslide inventories were used (Fig. 5). These were compiled by means of decades of field surveys, remote sensing and geophysical analysis in the study area.

Hereafter we report their description in detail:

- The "Rockslides and Rock Avalanches of Central Asia" (Strom and Abdrakhmatov, 2018): a large inventory including over 1000 polygons of large-scale (>=1 Mm^3) rockslides and rock avalanches, covering central Asian countries (except for Turkmenistan and Altai) plus Chinese Tien Shan and Pamir, and Afghan Badakhshan. Compiled in decades of field work and analysis of aerial/satellite imaging, it also comprises information on landslide morphometric parameters (runout, area), and 126 polygons on possible landslide bodies, dammed lakes, and head-scarps. Quantitative characteristics (area, volume, runout, etc.) for about 600 cases are provided as well.

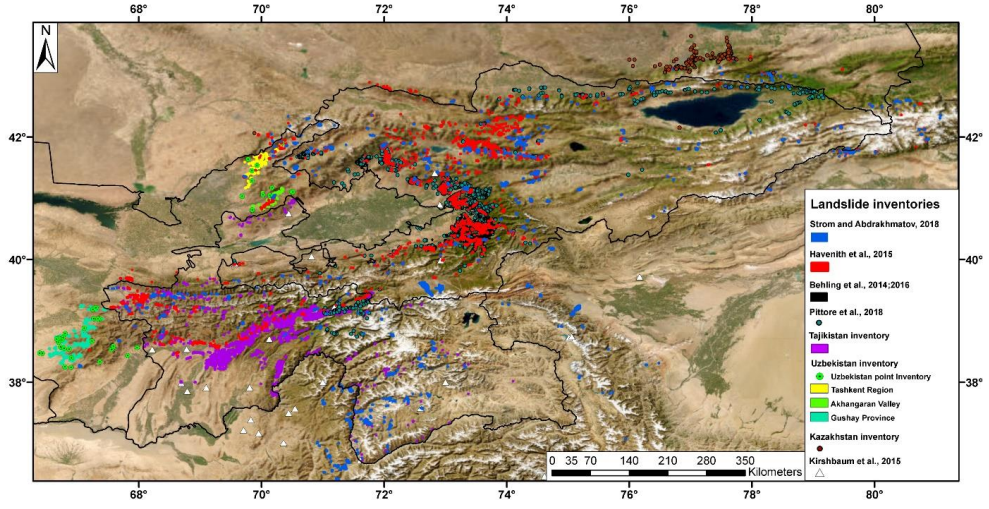

Figure 5. **Map of the adopted landslide inventory maps.** Basemap source: Esri, Maxar, Earthstar Geographics, and the GIS User Community.

- The "Tien Shan landslide inventory" (Havenith et al., 2015a): represents the largest inventory in the study area. Compiled by means of field surveys, remote sensing data interpretation and geophysical surveys, it

https://doi.org/10.5194/nhess-2023-33
Preprint. Discussion started: 28 February 2023

comprises the rockslides of the previous inventory together with other smaller landslides in soft sediments (Havenith et al. 2006a; Schlögel et al., 2011) for a total of 3,462 landslides polygons, also including information on landslide length and area.

- The "Multi-temporal landslide inventory for a study area in Southern Kyrgyz Republic derived from RapidEye satellite time series data (2009 – 2013)" (Behling et al., 2014; 2016; 2020), is a semi-automated spatiotemporal landslide inventory for the period from 1986 to 2013, covering a 2,500 km^2 in the Fergana valley rim in southern Kyrgyz Republic. This inventory includes 1,582 landslide polygons mapped from multi-sensor optical satellite time series data, together with information on spatiotemporal landslide activity patterns (area and year of trigger).
- "The EMCA landslide catalogue Central Asia" (Pittore et al., 2018), including 3,130 points, which covers mostly western and northern Kyrgyz Republic as well as Tajikistan's Region of Republican Subordination. The catalogue is a summary (point locations) of the documented landslides between 1954 and 2009 (Kalmetieva et al., 2009), which are collected by the Central Asian Institute for Applied Geosciences through geological surveys (field campaigns) on single sites close to urban areas.
- The "Tajikistan landslide database" provided by the Institute of Water problems, Hydropower, Engineering and Ecology of Tajikistan (IWPHE), which includes 2,710 landslide polygons and 114 landslide-prone areas (with information on length and area).
- The landslide inventory provided by the Institute of Seismology of the Academy of Science of Uzbekistan (ISASUZ), which covers the Tashkent province. It comprises a point inventory (including location, type, volume, length, and date of triggering; Nyazov R.A. 2020) and a polygon inventory digitized for this project from the maps in Juliev et al., 2017 (including a total 345 landslide polygons).
- The landslide inventory, provided by the LLP "Institute of Seismology" of the Science Committee of the Republic of Kazakhstan, covering mainly the Tien Shan area at the border with Kyrgyz Republic, and small part of the western Altai, including 254 point-objects with information on type, area/volume, triggering date.
- Part of the "Global Landslide Catalogue (GLC)" (Kirshbaum et al., 2015), which covers Kyrgyz Republic and Tajikistan, including 15 landslide point with a description on landslide size/type and triggering date/factor. The GLC was compiled since 2007 at NASA Goddard Space Flight Centre NASA and considers all types of mass movements triggered by rainfall, which have been reported in the media, disaster databases, scientific reports, or other sources.

3.2 Random Forest (RF) model

To generate the landslide susceptibility maps in this work, the Random Forest model (RF) was used. The RF is a nonparametric and multivariate machine learning technique, which was proposed by Breiman (2001), and first used in landslide susceptibility analysis by Brenning (2005). Since then, it has rapidly gained widespread consolidation through many research and case studies, as it is considered a relatively powerful approach in classification, regression, and unsupervised learning (Lagomarsino et al., 2017). Among the advantages of using the RF algorithm, there is the possibility of using numerical and categorical variables at the same time, without assumption on the statistical distribution of their values. Furthermore, RF is acknowledged to be capable of handling implicitly the multicollinearity of variables, identifying the uninfluential (or the detrimental) ones

https://doi.org/10.5194/nhess-2023-33
Preprint. Discussion started: 28 February 2023

Natural Hazards and Earth System Sciences
Discussions

(Breiman, 2001; Brenning, 2005). The RF also automatically performs a validation by building a Receiver Operating Characteristic Curve (ROC Curve) and calculates the relative Area Under the Curve (AUC). AUC is widely used as a quantitative indicator for the predictive effectiveness of susceptibility models: it can range from 0.5 (completely random predictions) to 1.0. This model, by means of the bootstrapping technique, also calculates the Out-of-Bag Error (OOBE) for each variable. This parameter measures the relative error that would be committed if a given variable is excluded from the RF classifier. OOBE can be used to assess the relative importance of each independent variable, thus representing a powerful tool to interpret the results and to rank the variables according to their importance (Catani et al., 2013). RF contains a series of binary tree predictors, which are generated by using a random selection of the input data (the independent variables which in LSM studies, are a set of physical parameters representing the predisposing factors), in order to split each binary node (yes/no), and to perform a classification of the target dependent variable (in LSM studies, the presence or absence of landslides). Some of the observations are used for internal testing to evaluate the predictive capability of each predictor tree. This information is used to iterate the procedure hundreds of times by growing other random trees (hence the name "Random Forest"), and to iteratively adjust the prediction effectiveness. Once the best predictor tree is identified, it is applied to the whole study area, to define the LSM. Another important key point of RF is that it has a great predictive performance and runs fast by summarizing many classification trees and this is particularly useful when dealing with large amounts of data.

3.3. Selection of independent variables

As independent variables, twenty "basic parameters" were selected in all 5 countries, based on the available data and according to the ones most widely adopted in literature (Catani et al., 2013; Reichenbach et al., 2018). Many of these are DEM-derived products (e.g., elevation, aspect, slope, slope curvature, flow accumulation, Stream Power Index, Topographic Wetness Index, Topographic Position Index). It must be considered that the resolution of the susceptibility maps depends on the resolution of the input data. Therefore, it was decided to use pixels corresponding to the MERIT DEM (Yamazaki et al. 2017) resolution (3" – ca. 90 m at equator and ca 70 m at 40° latitude). In addition, the DEM itself was used as a reference map, so that the other parameters were processed to have a perfect overlapping. Therefore, the resulting landslide susceptibility maps will also be perfectly overlapping to it. The variables such as lithology and soil type were rasterized with this resolution by choosing the most frequent value in a reference window. The twenty "basic parameters" used are listed below, including a brief description:

- MERIT DEM and DEM-derived products: Aspect, Slope Gradient, Total Curvature, Profile Curvature, Planar Curvature, Flow Accumulation, Topographic Wetness Index (TWI), Stream Power Index (SPI), Topographic Position Index (TPI).
- Lithology, derived from the geological map of the former Soviet Union made by the USGS (Persits et al. 1997).
- Soil type map from the DSMW database (Copernicus land use; https://land.copernicus.eu/).
- Distance from Faults: it is minimum distance, in meters, between each landslide and the nearest fault. The fault database is derived from the AFEAD catalogue (Styron and Pagani, 2020) and was modified after Poggi et al., a (in prep.).

https://doi.org/10.5194/nhess-2023-33
Preprint. Discussion started: 28 February 2023

Natural Hazards and Earth System Sciences
Discussions

- Distance from Roads: it is minimum distance, in meters, between each landslide and the nearest road. The roads database is derived from Scaini et al., (in prep.).
- Distance from Rivers: it is minimum distance, in meters, between each landslide and the nearest river. The river network database is derived from Coccia et al., (in prep.).
- Distance from Hypocentres: it is minimum distance, in meters, between each landslide and the nearest earthquake hypocentre with a magnitude greater than 6.5 (following the methodology adopted by Havenith et al., 2015a). The Hypocentre database was provided by Poggi et al., a (in prep.).
- Peak Ground Acceleration (PGA): 4 kind of PGA maps according to different return times (475 and 1000 years) and different materials (soil layers and bedrock) to which it refers were created (Poggi et al. b, in prep).

In addition to these "basic parameters", in this study it was decided to use five parameters related to the propensity of the territory to be affected by precipitation (Fig. 6). These parameters were obtained from the ERA5 database (www.ecmwf.int/en/forecasts/datasets/reanalysis-datasets/era5).

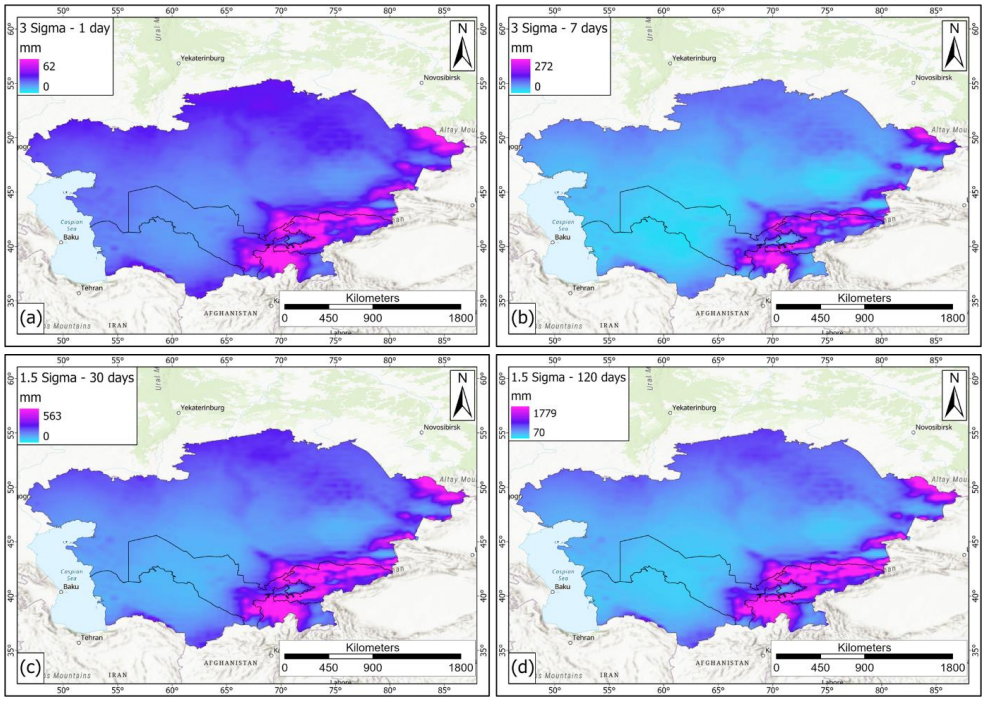

Figure 6. Rainfall maps from the ERA5 database (www.ecmwf.int/en/forecasts/datasets/reanalysis-datasets/era5). (a) rainfall amounts corresponding to 3 standard deviations for 1-day rainfall; (b) rainfall amounts corresponding to 3 standard deviations for 7-days rainfall; (c) rainfall amounts corresponding to 1.5 standard deviations for 30-days rainfall; (d) rainfall amounts corresponding to 1.5 standard deviations for 120-days rainfall. Basemap source: Esri, USGS, NOAA.

https://doi.org/10.5194/nhess-2023-33
Preprint. Discussion started: 28 February 2023


Natural Hazards and Earth System Sciences
Discussions

These data span from 1981 to 2020, have a 1-hour temporal resolution (summarized to daily resolution for this work) and a spatial resolution 0.25°. The first parameter is the Mean Annual Precipitation (MAP) map, where, for each pixel, the mean annual precipitation was calculated (Fig. 6). Other maps (named Sigma maps) have been calculated by the spatialization of the approach described in Martelloni et al (2011). In detail, for each rain gauge (represented by the pixels of ERA5 maps in this work) the rain values corresponding to a given standard deviation for several cumulative intervals are defined (e.g., the rain values corresponding to 2 standard deviations of the distribution of 3-days cumulative rainfall):

- Sigma 1.5 – 120 days: rainfall values corresponding to 1.5 standard deviations of the 120-days cumulative rainfall They range from 70 mm to 1778.8 mm (Fig. 6a).
- Sigma 1.5 - 30 days: rainfall values corresponding to 1.5 standard deviations of the 30-days cumulative rainfall. They range from 0 mm to 563.1 mm (Fig. 6b).
- Sigma 3 - 1 days: rainfall values corresponding to 3 standard deviations of daily cumulative rainfall. They range from 0 mm to 62.2 mm (Fig. 6c).
- Sigma 3 - 7 days: rainfall values corresponding to 3 standard deviations of the 3-days cumulative rainfall. They range from 0 mm to 271.9 mm (Fig. 6d).

The sigma parameters represent the probability of having a given rainfall amount over a defined time interval. In this work, four intervals were selected (1, 7, 30 and 120 days) to consider both short and long rain events, that can lead to the triggering of surficial or deep-seated landslides, respectively. For 1 and 7 days the maps of the rainfall values corresponding to 3 standard deviations over the mean rainfall were selected, to verify if short and very intense rainfall (with a very low probability of occurrence) could influence the slope stability in the study area. Regarding the 30-days and 120-days interval, rainfall values corresponding to 1.5 standard deviation were calculated, in order to assess the influence of longer and less intense rainfalls over slope stability.

3.4. Model optimization

The LSM was defined using the whole study area, instead of processing each country individually. This choice allowed to overcome the boundary effects associated with the use of independent countries. In addition, a buffer of 10 km was considered around the whole area, to avoid deformation due to boundary effects. These choices were helpful in reducing distortions and improving the quality of the results, but also led to a huge amount of data to be processed. Since the same resolution of the DEM was used for susceptibility assessment, the whole area was divided into about $1.07 * 10^9$ cells and for each cell 26 condition factors and 1 dependent variable were defined; this led to about $2.89 * 10^{10}$ data to be processed. In order to reduce the processing time and avoid computational problems due to the huge amount of data and to the width of the study area, large flat areas were filtered and not considered in the modelling process, since landslides generally take place along slopes (some exceptions to this statement in the area are represented by landslide around the flat Caspian Sea area (Pánek et al., 2016). For Turkmenistan no landslide database was available, so it was decided to train and test the model only with the other 4 countries, to obtain the best predictor model for the available data. The trained model has then been applied to the whole study area, including Turkmenistan, to define the LSM. Regarding the dependent variables, the landslides inventory was created by merging the data described in section 3.1. As a result, this landslide data was

https://doi.org/10.5194/nhess-2023-33
Preprint. Discussion started: 28 February 2023

Natural Hazards and Earth System Sciences
Discussions

quite heterogenous, hence an initial control and homogenization phase was necessary. In this framework the landslide data were checked to verify the presence of overlapping polygons or topological errors, which were removed. Since some landslide inventories were composed solely by points, these were mapped only as a "landslide points", a 100 m buffer was created around them, in order to include them in the model. However, when the points refer to large landslides, which are frequent in the study area, it is possible that part of the body of these landslides is still outside the perimeter achieved with the buffer. To avoid classifying these areas as non-landslide points, it was decided to create an additional buffer of 1 km around points, used as a mask where the non-landslide points were not to be selected. This process reduced the probability of pixels misclassification (e.g., landslide points considered as non-landslide points) during the training of the model. All the points inside the 1-km buffer were only considered during the model application, as well as point from Turkmenistan. Some landslide-prone areas were also present in the input inventories; since these were not real landslides but 'landslide-prone zones', these areas were not used to train the susceptibility model but were used in the validation of the results. This optimization procedure allowed to define an input dataset of $1.08*10^8$ points (along with 27 variables for each point) to be used to define the susceptibility model. A further optimization of the model was performed by the evaluation of the out of bag classification error, i.e., the variation of the misclassification probability with the number of grown classification trees. The classification error initially reduces with the increasing of classification trees, then it turns to be stable, so the definition of the optimal number of classification trees is required to avoid the use of an overgrown forest with an excessive number of trees (hence with high computational load and time) and without any advantage for the model (Fig. 7).

3.5. Model training

Once all the data were prepared and organized, the algorithm to create the landslide susceptibility maps was developed. A crucial step in LSM analysis is the approach used to sample the variables to train and validate the model. As in any other statistical procedures, the size of the dataset influences the results, therefore the higher the number of samples to perform the statistical calibration/validation of the model, the more reliable are the obtained results. To avoid a generalized hazard overestimation, Catani et al. (2013) demonstrated that a random sampling improves the predictive capability of the map, and that the susceptibility model should also be trained/validated with respect to information about non-landslide locations. Regarding the proportion between the calibration and validation dataset samples, it is common practice to split them according to a 70/30 ratio. Therefore, using ESRI ArcGIS Pro software, all the variables were sampled pixel by pixel, after which, with the Matlab software, from the total of the sampled points, all the points within a landslide and a same amount of randomly chosen non-landslide points were extracted. This input dataset was divided into two parts, 70% of the data (calibration dataset) was used for the training phase, and the remaining 30% (validation dataset) for the testing phase. The selection and division were randomly repeated 5 times, in order to assess the stability of the model to the variation of the training and testing datasets, hence, to verify the absence of overfitting issues. Each one of these datasets was created to be equally composed by pixel within a known landslide and pixel outside a landslide. All these data were then used to train and test the algorithm created to predict the landslide susceptibility of the whole area.

https://doi.org/10.5194/nhess-2023-33
Preprint. Discussion started: 28 February 2023

Natural Hazards and Earth System Sciences
Discussions

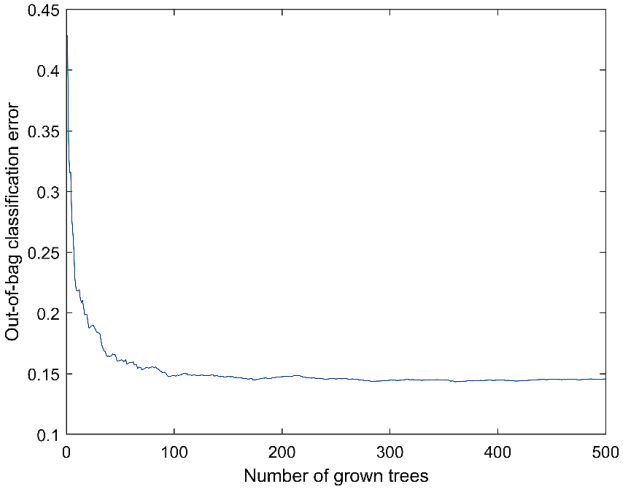

Figure 7. Example of out of bag classification error. The error is stable using 100 or more trees.

The best predictor model identified in the training phases was then applied to all the available data (also for Turkmenistan and for the 1-km buffer area around the point-object landslides) for the development of the susceptibility map on the whole Central Asia area. The results obtained from the application of the aforementioned methodology are the susceptibility map, the ROC (Receiver Operating Characteristic) curves with their AUC (Area Under the Curve) values, and the histogram of the importance of variables. ROC and AUC are used to verify the quality of the landslide susceptibility model, both by graphical and analytical approach. Due to the high volume of data, their variety, values, and heterogeneity a specific algorithm was created for this work, that was set to be able to perform several activities:

- Reading and properly formatting the input data and then dividing them between independent and dependent variables.
- Automatically and randomly selecting locations associated with landslides or outside landslides to create the training and test datasets.
- Identifying the best predictor and evaluating its performances by the calculation of the misclassification probability of the values calculated by the model.
- Evaluating the overall performances of the model by the mean of ROC and AUC.
- Identifying the importance of the parameters in landslide susceptibility.
- Applying the model to the whole study area, calculate the probability of classification (landslide or non-landslide) of each pixel and extraction of the final map in raster format.

The algorithm was set to work in classification mode, e.g., for each pixel a value (1 or 0) is assigned to identify the presence or absence of a landslides (dependent variable), along with the values of the independent variables. Using these data, the RF model identifies the best association of independent variables linked to presence or absence of landslides (landslide susceptibility prediction model).

https://doi.org/10.5194/nhess-2023-33
Preprint. Discussion started: 28 February 2023

Natural Hazards and Earth System Sciences
Discussions

The prediction model is then applied to all the pixels of the investigated area, and the probability of each pixel to be classified as landslide (or non-landslide) pixel is evaluated. These probability values are those used to create the landslide susceptibility maps. It must be noticed that the landslide inventories adopted to train the RF rarely reported the type of landslide, so the LSMs must be considered not related to a specific type of landslide.

3.6. Model validation

To verify the quality of the susceptibility models, beside the AUC value previously reported, a confusion matrix for the four countries where the model was trained was created (Fig. 8). In each matrix the predicted landslide classes are compared with the ground truth to verify the presence of significant misclassification error. In all the matrix the value 1 represent the presence of landslide, the value 0 represents the absence of landslides; the numbers in each cell represent the number of pixels classified in that combination of 0 and 1, according to this scheme (the first number represent the predicted class, the second number the ground truth):

- 0-0 (True negative): pixels outside any landslides are correctly identified as no-landslide pixels by the model.
- 1-1 (True positive): pixels inside a landslide are correctly identified as landslide pixels by the model.
- 0-1 (False negative): pixels inside a landslide are wrongly identified as no-landslide pixels by the model.
- 1-0 (False positive): pixels outside any landslides are wrongly identified as landslide pixels by the model.

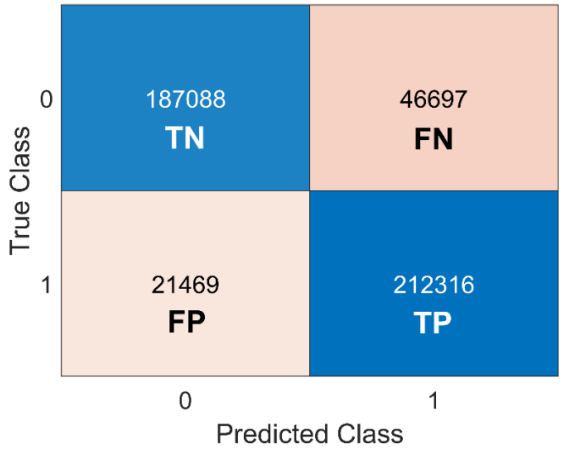

Figure 8. Confusion matrix for the four countries where the model was trained.

The 0-0 and 1-1 combinations represent well classified pixels (blue cells in Fig. 8), while 0-1 and 1-0 represent misclassification error (light red cells in Fig. 8). Since this matrix needs some ground-truth parameters (True classes), it can be applied only where the presence or absence of landslides is known. For this reason, in this work, this matrix was calculated considering only the test dataset. A further control of the results was made using the areas prone to landslides identified in the used landslide inventories.

https://doi.org/10.5194/nhess-2023-33
Preprint. Discussion started: 28 February 2023

Natural Hazards and Earth System Sciences
Discussions

3.7. Landslide susceptibility and elements at risk

The susceptibility map of the study area was intersected with the elements at risk, consisting of roads-railways, population, to analyse the landslide susceptibility distribution in the area covered by elements at risk. The database of element at risk was provided by Scaini et al., in prep. In order to perform the analysis several approaches were defined based on the different types of elements at risk. the population and buildings data were based on a grid with a spatial resolution of 1km^2, defining for each cell the number of inhabitants, the number of different types of buildings (residential, commercial, industrial, education and healthcare), and the mean susceptibility class by means of spatial statistics between input databases (population-buildings data and susceptibility map). The results carried out from the spatial statistics allowed to assess the people and buildings distribution within each susceptibility class. On the contrary, the linear elements (roads and railways) were divided in segments with 1-km in length, and buffered, setting a distance parameter equal to 100 m. After this preliminary process, the spatial statistics with the landslide susceptibility have been carried out.

4. Results

4.1 Susceptibility map

In the map presented in the following Figures 9 and 10, the susceptibility values, ranging from 0 to 1, were classified into five classes (Table 2). Here the corresponding extension and percentage of the study area are also reported, showing that the most frequent susceptibility class for the whole study area is the null class (=87.8%; landslides generally don't occur in flat areas), followed by low and medium classes. Only the 4% of the central Asian territory is represented by areas with high and very high landslide susceptibility (Table 2).

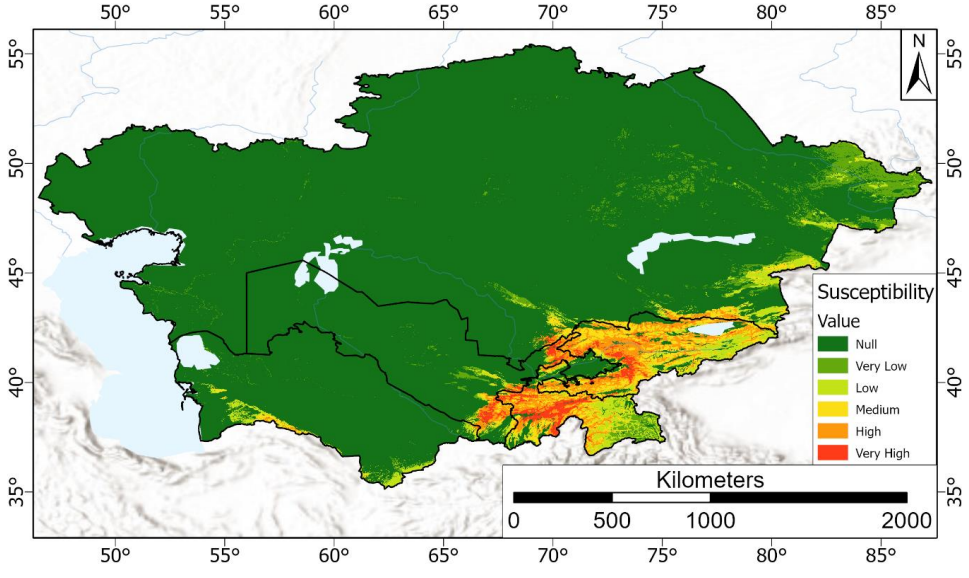

Figure 9. Landslide susceptibility map of Central Asia. Basemap source: Esri, USGS, NOAA.

https://doi.org/10.5194/nhess-2023-33
Preprint. Discussion started: 28 February 2023

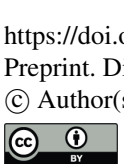

Natural Hazards and Earth System Sciences
Discussions

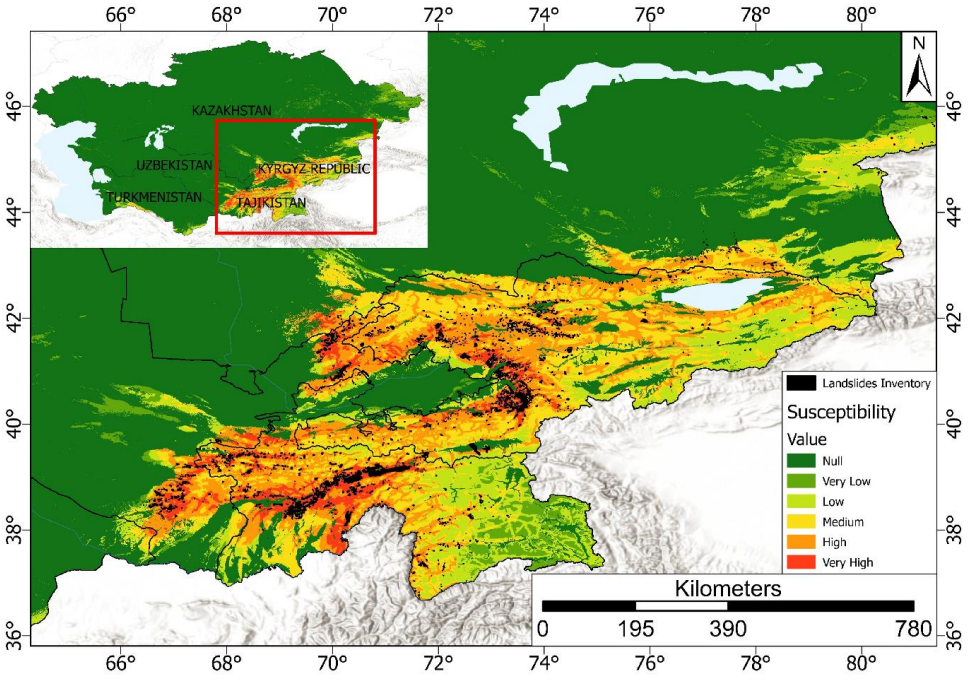

Figure 10. Detail of the landslide susceptibility map with the overlapping landslide polygons (in black). On the top left the detailed area with respect to the central Asian territory. Basemap source: Esri, USGS, NOAA.

Table 2. Landslide susceptibility class intervals, corresponding area, and percentage with respect to CA.

Susceptibility class	Landslide spatial probability interval	Corresponding area (km^2)	Corresponding percentage of CA (%)
Null	0 - 0.05	2,889,481.2	87.8
Very Low	0.05 - 0.25	94,674.7	2.9
Low	0.25 - 0.35	85,294.1	2.6
Medium	0.35 - 0.45	87,528.5	2.7
High	0.45 - 0.6	99,689.8	3
Very High	0.6 - 1	31,436.4	1

In Fig. 11, the susceptibility maps of five selected areas are displayed. From these details it is possible to ascertain the high usefulness of the landslide susceptibility map realized by applying the Random Forest model, which, mainly based on the hydro-geomorphological properties, can establish the degree of susceptibility even in areas where there is no awareness of the predisposition to instability due to the absence of reported landslides. In particular:

https://doi.org/10.5194/nhess-2023-33
Preprint. Discussion started: 28 February 2023

Natural Hazards and Earth System Sciences
Discussions
Open Access
EGU

- Fig. 11a shows the area north of the city of Denau, in the south-east of Uzbekistan, which is characterized by a high susceptibility, despite the almost total absence of mapped landslides.
- Fig.11b shows a detail of the city of Ura-Tube, in the North-West of Tajikistan, where there are not any known landslides, but a high susceptibility has been obtained in the surrounding mountain relief.
- In Fig. 11c there is a close-up on the city of Dushanbe, the capital of Tajikistan, where close to roads and inhabited centres a high landslides susceptibility is observed.
- The shores of Lake Issyk-Kul in the Kyrgyz Republic, shown in Fig. 11d, are generally flat areas, with a low or null landslide susceptibility but in the central zone.
- Finally, Fig. 11e shows a detail of the western area of the Kyrgyz Republic, where a high landslide susceptibility is observed along the slopes adjacent to the river network.

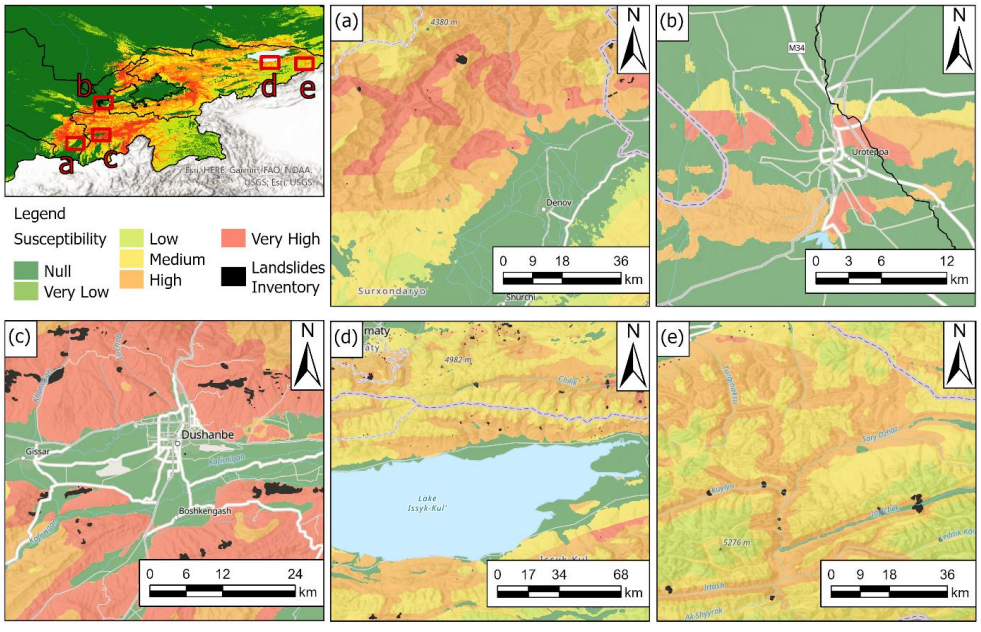

Figure 11. Details of the landslide susceptibility map. (a) the city of Denau, Uzbekistan; (b) the city of Ura-Tube, Tajikistan; (c) the city of Dushanbe, Kyrgyz Republic; (d) the Lake Issyk-Kul, Kyrgyz Republic; (e) the eastern area of the Kyrgyz Republic. Black poligons represent landslide areas from the adopted landslide inventories. Basemap source: Esri, USGS, NOAA.

4.2 The Fergana valley mountainous rim

The Fergana valley spreads across eastern Uzbekistan, southern Kyrgyz Republic, and northern Tajikistan (Fig. 12). It is one of the largest intermountain depressions in Central Asia, located between the mountain systems of the Chatkal-Kuraminsk ranges in the north and the Turkestan--Alai in the south. The two main rivers, the Naryn and the Kara Darya, flow into the valley and unite forming the Syr Darya. In this area landslides represent one of the major natural hazards due to their frequent (seasonal) occurrence across large areas: in fact, they are particularly

https://doi.org/10.5194/nhess-2023-33
Preprint. Discussion started: 28 February 2023

Natural Hazards and Earth System Sciences
Discussions

concentrated in a range of altitudes between 700 and 2000 m along the topographically rising rim below its transition into higher mountainous terrain (Roessner et al., 2000; 2004; 2005; Behling et al., 2014; 2016). This region is quite densely populated, and landslides lead almost every year to damage of settlements and infrastructure and loss of human life (Schloegel et al., 2011; Piroton et al. 2020). In this area landslide activity is caused by complex interactions between tectonic, geological, geomorphological and hydrometeorological factors (Havenith et al., 2015a, b). In the Fergana valley rim mass movements are often characterized by deep and steep scarps, mobilize weakly consolidated sediments of Tertiary or Quaternary age, including loess deposits (Piroton et al., 2020). These kinds of landslides are particularly deadly, and can be triggered by a combination of long-term slope destabilization factors (e.g., rainfall and snowmelt) and short-term triggers (Danneels et al., 2008). Slope landslide susceptibility was analysed in this area using the previously mentioned methodologies. Fig. 12 shows the particular about the landslide susceptibility map obtained for the Fergana Valley, while Fig. 13 reports the histogram of the area occupied by each susceptibility class. It can be observed that the most frequent susceptibility class in the Fergana Valley area is the Null class, which covers an area of about 20,743 km^2, that is 36% of the valley. The Very Low and Low classes occupy respectively an area of 681 km^2 (1.2%) and 5,431 km2 (9.4%). The Medium class instead extends for about 8,608 km2, namely the 15% of the total. The High class instead extends for about 16,395 km^2, that is 28.5% of the total and finally, the remaining 9.9% of the national territory, that is about 5,683 km^2, is classified in the Very High class.

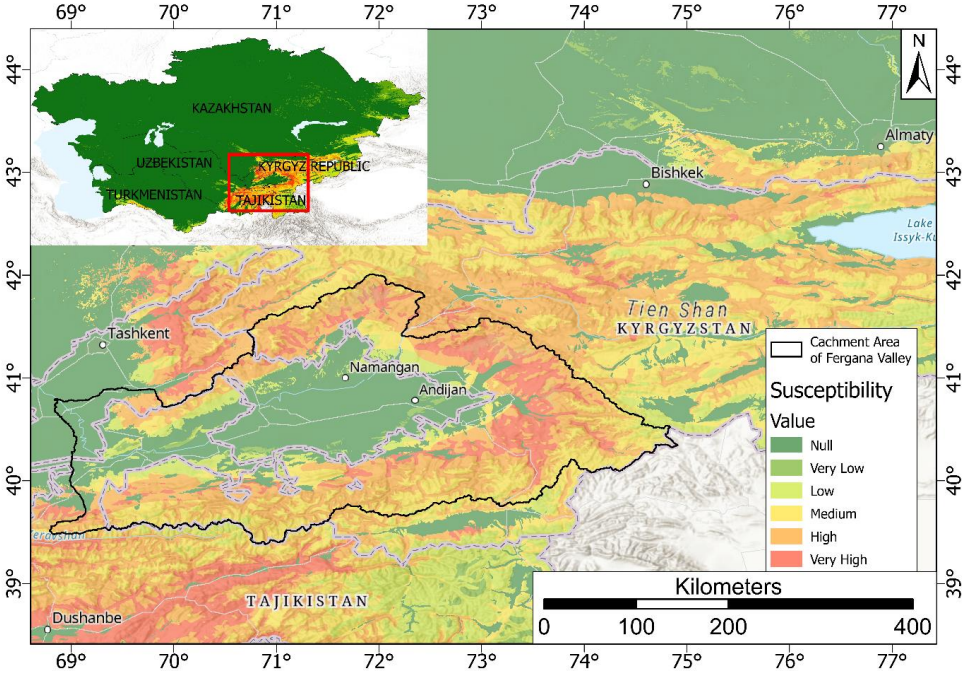

Figure 12. Detail of the landslide susceptibility map obtained for the Fergana Valley. Basemap source: Esri, USGS, NOAA.

https://doi.org/10.5194/nhess-2023-33
Preprint. Discussion started: 28 February 2023

Natural Hazards and Earth System Sciences
Discussions

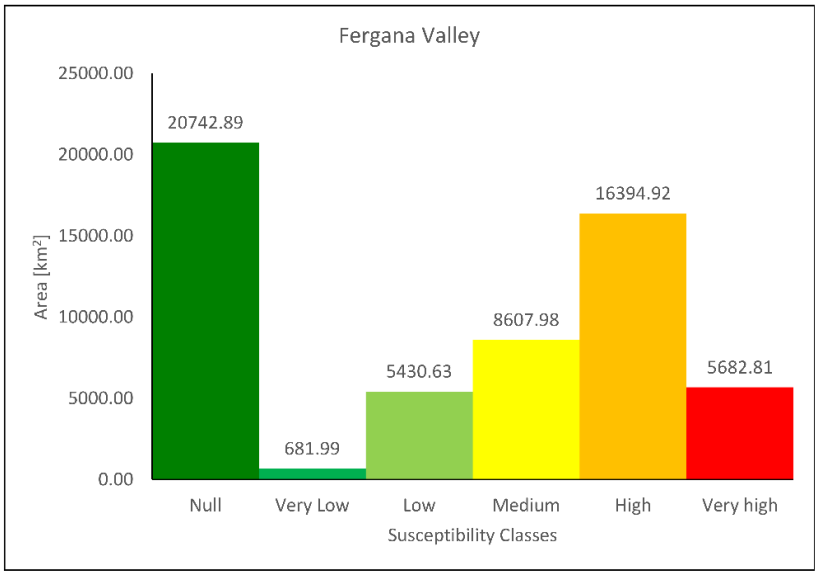

Figure 13. Frequency histogram of susceptibility classes obtained for the Fergana Valley mountainous rim. On each bar the corresponding area in km² is reported.

4.3 Trained model performances and conditioning factors relevance

The RF was initially trained setting 1,000 trees to be growth. After the first run, the analysis of the out-of-bag error revealed that misclassification probability reduced significantly with a forest of 150 trees and then reduced slightly up to 500 trees, then it turned to be stable, so the optimal number of trees was set equal to 500 and used for all the simulations. As described above, the model was run 5 times to verify its stability and the AUC values ranged from 0.93103 to 0.93144 (Fig. 14), with a mean value of 0.93122 and a standard deviation of 0.00015. The low variance of the AUC values confirmed the stability of the model and its applicability to the whole area. As we can see in the ranking of the susceptibility parameters, reported in Fig. 15, soil type, lithology, elevation, the distance from roads and hypocentres plays a crucial role in landslide susceptibility, since they are the five most influencing factors (for the four countries where the model was trained). Rainfall parameters are also important in the obtained landslide susceptibility, in particularly the 1-day rainfall value that shows the highest importance among the rainfall parameters. Also, the PGA maps are a relevant factor, while TWI and slope curvature are the less important parameters. The average AUC value of the models is 0.93122, indicating their very good quality. Such high AUC values can indicate the presence of overfitting issues, but this hypothesis can be discarded, since the random variable resulted without any importance in landslide susceptibility (negative OOBE value).

https://doi.org/10.5194/nhess-2023-33
Preprint. Discussion started: 28 February 2023

Natural Hazards and Earth System Sciences
Discussions

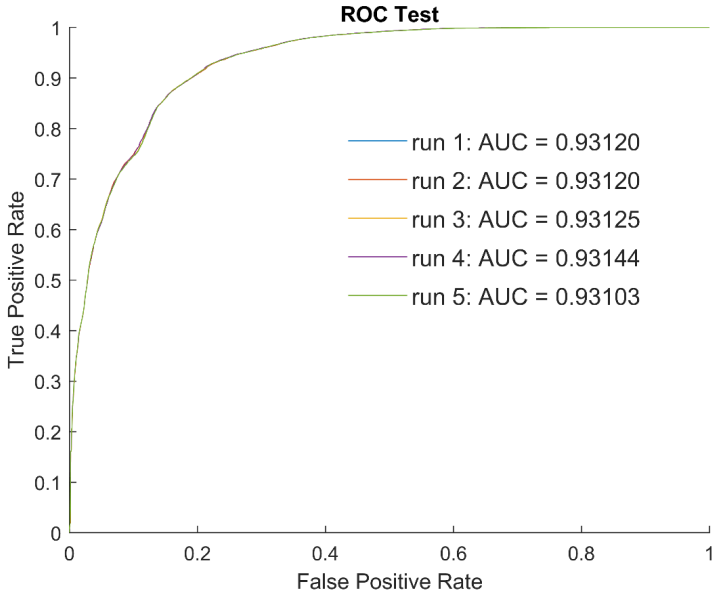

519

520 **Figure 14. ROC curve and relative AUC value for each model run.**

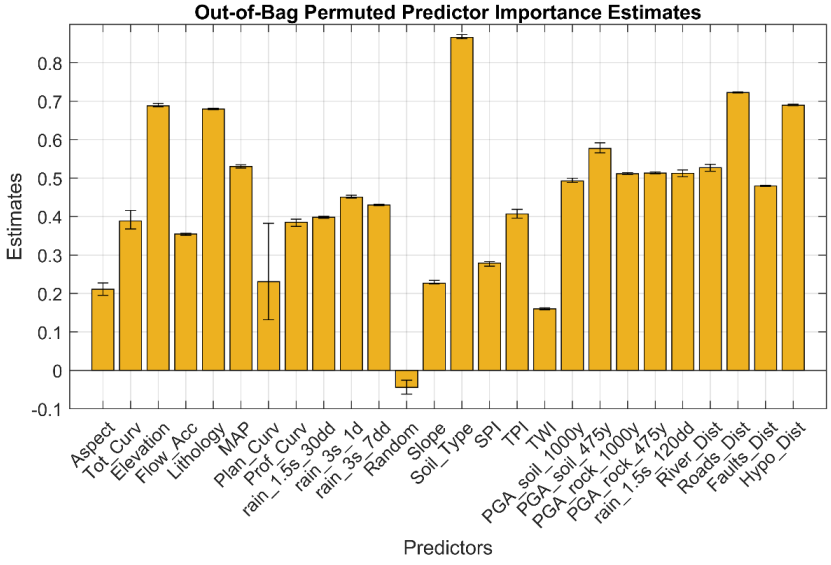

521

522 **Figure 15. Variable importance in landslide susceptibility for the four countries where the model was**
523 **trained**. From the 5 model runs, the results were averaged and displayed in this image, with the error bars showing
524 the maximum and the minimum value obtained.

https://doi.org/10.5194/nhess-2023-33
Preprint. Discussion started: 28 February 2023

Natural Hazards and Earth System Sciences
Discussions

4.4 Landslide susceptibility and exposed elements

Concerning the outcomes regarding buildings and population, they are represented by Table 3, in which for each susceptibility class the number of people and the number of different building types are reported, and in the bar diagram of (Fig. 16). The obtained results about roads and railways are reported in Table 4 and in Fig. 17.

Table 3. Population and buildings distribution in each landslide susceptibility class.

Element at risk	Landslide susceptibility				
	Null	Low	medium	high	very high
Population	68,422,152	3,046,892	1,612,487	2,812,081	97,934
Residential buildings	8,769,270	319,776	245,754	386.628	12,753
Commercial buildings	2,196,037	103,745	68,187	68.232	3,410
Industrial buildings	705,352	14,776	6396	7024	110
Education buildings	42,472	1802	960	2102	96
Healthcare buildings	15,476	224	84	226	2

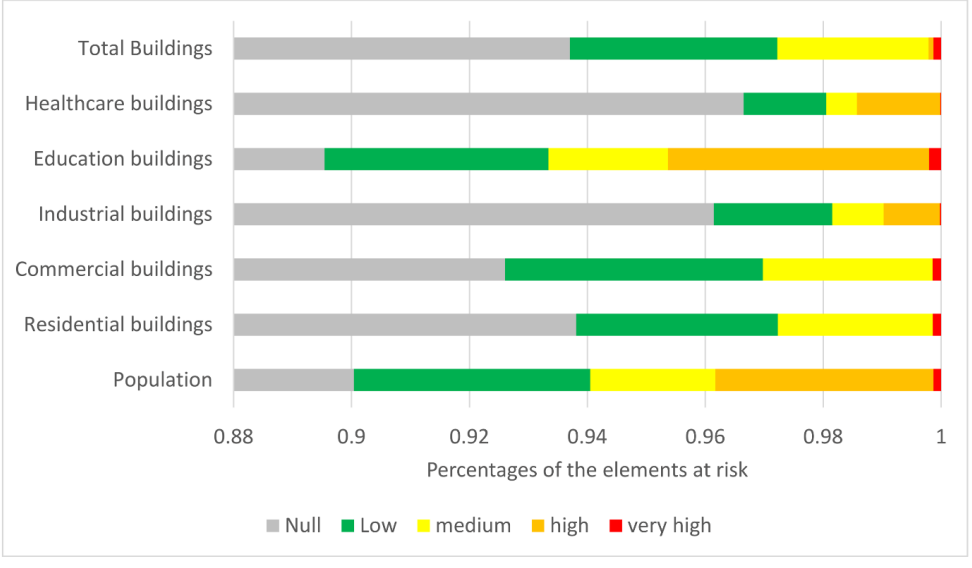

Figure 16. Percentage of the Element at risk falling within landslide susceptibility classified areas.

https://doi.org/10.5194/nhess-2023-33
Preprint. Discussion started: 28 February 2023

Table 4. Distribution (corresponding km) of road and railway classes in landslide susceptibility classes.

		Null	Low	Medium	High	Very High
Road Class	Primary	15,000	646	368	873	26
	Secondary	28,773	911	589	1,173	30
	Tertiary	71,515	2,637	1,643	3,898	55
	Trunk	30,058	1,887	686	1,887	77
	Motorway	1,732	/	/	/	/
Railway Class	High-Speed	45,866	589	317	187	25
	Conventional	128	4	16	12	/

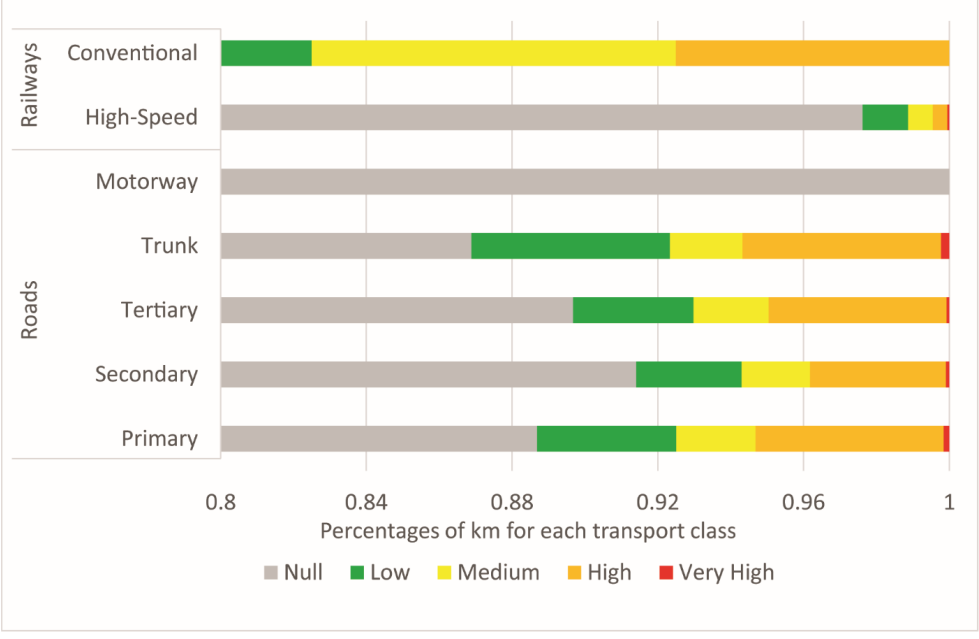

Figure 17. Landslide susceptibility distribution for each transportation class.

5. Discussion

Landslide susceptibility

The main issue affecting the used random forest model is the need of an adequate training dataset to properly calibrate the predictor model. The first step of the work has been the homogenization of the landslide data, the used landslide inventory was created starting from different sources, hence, with quite non-homogeneous (e.g., in some cases the whole landslide perimeter was available, in other cases only a point representing the source area

https://doi.org/10.5194/nhess-2023-33
Preprint. Discussion started: 28 February 2023

of each landslide was provided, without info about the landslide dimension or propagation distance; more in general there were few or no data about the landslide type or triggering causes). The lack of some data about the landslides, or the partial or complete lack of landslides as in Kazakhstan and Turkmenistan, could lead to underestimate the real landslide hazard of the studied countries, since some points could have been wrongly classified (e.g., they have been considered as no landslide areas, but it was possible that a not reported landslide was present). Furthermore, not all the adopted landslide inventories included information regarding the landslide types, leading to the creation of a general landslide susceptibility map, where all the types of landslides are considered. The created maps have been validated only using the available landslide dataset, providing good results and highlighting the good prediction capability of the model. Anyway, an in-situ validation in some sample areas can help to verify the quality of the results. As previously stated, for Turkmenistan there was no landslide inventory available to train the RF model, therefore the corresponding LSM was obtained applying the model trained for the other four countries. The lack of landslide data did not allow any validation of the result or estimation of the quality of the susceptibility map of Turkmenistan. Furthermore, applying the model developed for the other countries, the same importance of the conditioning factors (e.g., the independent variables) was assumed. For these reasons, the landslide susceptibility map for Turkmenistan is more uncertain than those evaluated for the other four countries. Among the used conditioning factors, soil type, distance from roads and distance from hypocentres resulted to be the most influencing factors in slope stability, while planar curvature resulted with a high variability of its importance. These parameters have been hence more deeply analysed to understand how the influence landslide susceptibility. According to the partial dependency plots (Fig. 18), which show how the values of each conditioning factor influence the landslide susceptibility, the soil types more related to landslides are lithosols and cambisols, low thickness soils limited in depth by a continuous coherent and hard rock layer, located in steeply slopes, with more than 30% of slope gradient. While the classes that have the lowest importance score are fluvisols (young soils in alluvial deposits), xerosols (mainly arid clay) and chernozems (soils rich in organic matter), each situated in flat to hilly areas, with less than 30% of slope gradient. Distance from roads, as expected, is important for low values since the importance score is maximum for distance close to zero and it decrease exponentially with the increasing of the distance. A similar behaviour can be noted with the distance from hypocentres, meaning that areas close to hypocentres (within a radius of about 25 km) can more easily experience landslide phenomena in case of future earthquakes. The partial dependency plot of planar curvature showed that the variability highlighted in Fig. 16, is in fact, not so relevant since the range of the importance score is quite limited (values ranging from 0.4992 to 0.5008). In addition, it is possible noticing that negative values of planar curvature have a higher importance score than zero values or positive values, meaning that concave slopes are more prone to landslide than plain or convex surfaces.

Landslide susceptibility and exposed elements

The integration of susceptibility map with the maps of element al risk and communication router allowed to identify those elements potentially more prone to landslide hazard, even of with some limitations. The obtained results are indeed influenced by the input data (the susceptibility maps and the elements at risk databases).

https://doi.org/10.5194/nhess-2023-33
Preprint. Discussion started: 28 February 2023

Natural Hazards and Earth System Sciences
Discussions

583 The buffering procedures on roads and railways could overestimated or underestimated the susceptibility
584 distribution in some cases, likewise the analysis at 1km^2 resolution on population and buildings could led to an
585 exaggeration in the assessment of elements distribution in each class of landslide susceptibility.

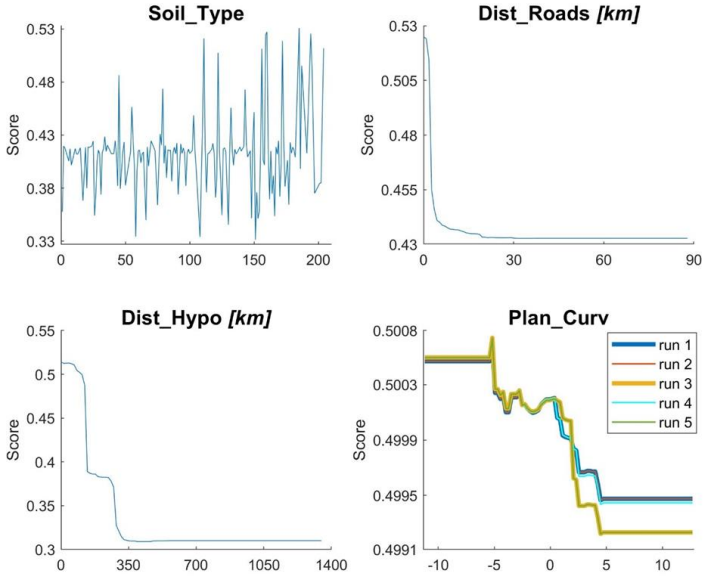

586

587 **Figure 18. Partial dependence plots.**

588 Nevertheless, the adopted approaches represented the only way to obtain an analysis as much accurate as possible
589 respect to the input databases. In this perspective, the detail of analyses could be improve focusing both on the
590 refinement of the analysis resolution (e.g., population and buildings) and on the elements at risk that are not located
591 in flat areas, where the landslide susceptibility is surely 0 or NULL.

592 **6. Conclusions**

593 In this work a new landslide susceptibility assessment of Central Asia was carried out. With respect to previous
594 works, in this research a unique map was created and with a higher resolution, in order to avoid boundary effects,
595 to get to more homogeneous and with better resolution results. The used approach allowed also to identify the
596 most relevant landslides predisposing factors: soil type distance from roads and hypocentres. The size and the
597 heterogeneity of the study area required the use of many input variables, some of them never used before in
598 landslide hazard assessment, and the elaboration of a high volume of data, as well as the adoption of some specific
599 procedure to accounting for the presence of heterogeneities and uncertainties in the input data, as the presence of
600 point landslides. The comparison with elements at risk and communication routes allowed a better assessment of
601 landslide hazard in the area, which can be useful to improve the land use management and to reduce the risk. The
602 main limitation of the work is related to absence of data about type and geometry for several landslides; in the
603 future a better input landslide inventory could help get to different susceptibility maps for different landslide types.

https://doi.org/10.5194/nhess-2023-33
Preprint. Discussion started: 28 February 2023

Another limitation is due to the absence of any information about the presence or absence in Turkmenistan, which did not allow any clear validation of the results for this country.

Code and data availability. The landslide susceptibility model was implemented by using the cited landslide inventory maps, published by the following authors: Behling et al., 2014, 2016, 2020; Havenith et al., 2015a; Kirshbaum et al., 2015; Pittore et al., 2018; Strom and Abdrakhmatov, 2018. Other data implemented in the model, such as MERIT DEM, geological formations, Active Fault Database, soil type map, rainfall maps are available from Yamazaki et al. 2017, Persits et al., 1997, Styron and Pagani, 2020, https://land.copernicus.eu/, www.ecmwf.int/en/forecasts/datasets/reanalysis-datasets/era5, respectively. The database on infrastructures, river network, PGA and other landslide inventories were provided by the SFRAAR project partners: RED (Risk, Engineering + Development – Pavia, Italy), OGS (National Institute of Oceanography and Experimental Geophysics, Seismological Research Center, Trieste, Italy), IWPHE (Institute of Water problems, Hydropower, Engineering and Ecology, Dushanbe, Republic of Tajikistan), ISASUZ (Institute of Seismology of the Academy of Science of Uzbekistan, Tashkent, Uzbekistan), LLP (Institute of Seismology of the Science Committee of the Republic of Kazakhstan, Almaty).

Author contribution. Ascanio Rosi implemented the landslide susceptibility model, William Frodella conceived with Ascanio Rosi the article structure and collected the data, Nicola Nocentini prepared the landslide susceptibility data and supported the model implementation, Francesco Caleca prepared the infrastructure data for the model implementation and performed the statistical analysis involving the landslide susceptibility areas and the exposed elements. All the above mentioned authors contributed to the writing of the article and the figure graphics. Hans Balder Havenith and Alexander Strom provided the landslide databases from: i) Havenith, H.B., Strom, A., Torgoev, I., Torgoev, A., Lamair, L., Ischuk, A., Abdrakhmatov, K.: Tien Shan geohazards database: Earthquakes and landslides. Geomorphology 249, 16–31, 2015a; and ii) Strom, A., Abdrakhmatov. K.: Rockslides and rock avalanches of Central Asia: distribution, morphology, and internal structure. Elsevier, 441pg. ISBN: 978-0-12-803204-6, 2018. They also provided the landslide pictures for figures 3 and 4, and critically reviewed the paper. Veronica Tofani coordinated the work and reviewed the paper.

Competing interests. The contact author has declared that none of the authors has any competing interests.

Acknowledgements. This work was developed within World Bank-funded project "*Strengthening Financial Resilience and Accelerating Risk Reduction in Central Asia*" (SFRARR), in collaboration with the European Union, and the GFDRR (Global Facility for Disaster Reduction and Recovery), with the goal of improving financial resilience and risk-informed investment planning in the central Asian countries (Kazakhstan, Kyrgyz Republic, Tajikistan, Turkmenistan and Uzbekistan). This work represents the outcomes of the Task 7 "Landslide Scenario Assessment", coordinated by the UNESCO Chair on Prevention and Sustainable Management of Geo-Hydrological Hazards (University of Florence). In particular, the authors would like to thank Gabriele Coccia and Paola Ceresa from Red Risk Engineering (Pavia, Italy) for providing river network data and for the valuable coordination and constant support, as well as Valerio Poggi and Chiara Scaini from OGS (National Institute of Oceanography and Experimental Geophysics, Seismological Research Center, Trieste, Italy) for providing seismic

https://doi.org/10.5194/nhess-2023-33
Preprint. Discussion started: 28 February 2023

data (active faults, Pga) and exposure data. We would also like to thank the partners from Central Asia for the fruitful collaboration, in particular: IWPHE (Tajikistan), ISASUZ (Uzbekistan) and LLP (Kazakhstan,).

References

Abdrakhmatov, K. Y., Aldazhanov, S. A., Hager, B. H., Hamburger, M. W., Herring, T. A., Kalabaev, K. B., Makarov, P. Molnar, S. V. Panasyuk, M. T. Prilepin, R. E. Reilinger, I. S. Sadybakasov, B. J. Souter, Yu. A. Trapeznikov, V. Ye. Tsurkov Zubovich, A. V. Relatively recent construction of the Tien Shan inferred from GPS measurements of present-day crustal deformation rates. Nature, 384(6608), 450-45319, 1996.

Abdrakhmatov, K., Havenith, H.B., Delvaux, D., Jongmans, D., Trefois, P.: Probabilistic PGA and Arias Intensity Maps of Kyrgyz Republic (Central Asia). J. Seismol. 7.2: 203-220, 2003.

Akgun, A. A.: comparison of landslide susceptibility maps produced by logistic regression, multi-criteria decision, and likelihood ratio methods: A case study at İzmir, Turkey. Landslides, 9, 93–106, 2012.

Bazzurro, P. et al.: Strengthening Financial Resilience and Accelerating Risk Reduction in Central Asia - the SFRARR project. The SFRARR probabilistic flood hazard assessment. In prep. for the Special Issue "Regionally consistent risk assessment for earthquakes and floods and selective landslide scenario analysis in Central Asia". Natural Hazards and Earth System Sciences (NHESS).

Behling, R., Roessner, S., Kaufmann, H., Kleinschmit, B.: Automated spatiotemporal landslide mapping over large areas using rapideye time series data. Remote Sens. 6, 8026–8055, 2014.

Behling, R., Roessner, S., Golovko, D., Kleinschmit, B.: Derivation of long-term spatiotemporal landslide activity—A multi-sensor time series approach. Remote Sens. Environ. 186, 88–104, 2016.

Behling, R., Roessner, S.: Multi-temporal landslide inventory for a study area in Southern Kyrgyz Republic derived from RapidEye satellite time series data (2009 – 2013). V. 1.0. GFZ Data Services. https://doi.org/10.5880/GFZ.1.4.2020.001, 2020.

Brabb, E.E.: Innovative approaches to landslide hazard mapping, in: Proceedings 4th International Symposium on Landslides, Toronto, 1, 307–324, 1984.

Breiman, L.: Random forests. Mach. Learn. 45, 5–32, 2001.

Brenning, A.: Spatial prediction models for landslide hazards: Review, comparison and evaluation. Nat. Hazard Earth Syst, 5, 853–862, 2005.

CAC DRMI: Risk assessment for Central Asia and Caucasus: desk study review, 2009.

Carrara, A.: Multivariate models for landslide hazard evaluation. J. Int. Assoc. Math. Geol. 15, 403–426, 1983.

Cascini, L.: Applicability of landslide susceptibility and hazard zoning at different scales. Eng. Geol., 102 (3-4):164–177, 2008.

Catani, F., Lagomarsino, D., Segoni, S., Tofani, V.: Landslide susceptibility estimation by random forests technique: sensitivity and scaling issues. Nat. Hazards Earth Syst. Sci. 13, 2815, 2013.

https://doi.org/10.5194/nhess-2023-33
Preprint. Discussion started: 28 February 2023

673 Chedia, O.K., Lemzin, I.N.: Seismogenerating faults of the Chatkal depression. In: Seismotectonics and seismicity
674 of the Tien Shan. Frunze, Ilim, 18–28, 1980.

675 Chen, L., Van Westen, C.J., Hussin, H., Ciurean, R.L., Turkington, T., Chavarro-Rincon, D., Shrestha, D.P.:
676 Integrating expert opinion with modelling for quantitative multi-hazard risk assessment in the Eastern Italian
677 Alps. Geomorphology, 273 (15):150–167, 2016.

678 Coccia, G. et al.: The SFRARR probabilistic flood hazard assessment. In prep. for the Special Issue "Regionally
679 consistent risk assessment for earthquakes and floods and selective landslide scenario analysis in Central
680 Asia". Natural Hazards and Earth System Sciences (NHESS).

681 Corominas, J., Copons, R., Vilaplana, J.M., Altimir, J., Amigó, J.: Integrated landslide susceptibility analysis and
682 hazard assessment in the principality of Andorra. Nat. Hazards, 30 (3): 421–435, 2003.

683 Cruden, D.M., Varnes, D.J.: Landslide types and processes. Landslides: Investigation and Mitigation. Special
684 Report 247, Transportation Research Board, Washington, 36–75, 1996.

685 Danneels, G., Bourdeau, C., Torgoev, I., Havenith, H. B. Geophysical investigation and dynamic modelling of
686 unstable slopes: case-study of Kainama (Kyrgyzstan). Geophysical Journal International, 175(1), 17-34,
687 2008.

688 Delvaux, D., Abdrakhmatov, K.E., Lemzin, I.N., Strom, A.L.: Landslides and surface breaks of the 1911 Ms 8.2
689 Kemin earthquake, Kyrgyzstan, Russian Geology and Geophysics, 2001, 42, 10, 1667-1677, 2001.

690 Duman, T.Y., Can, T., Gokceoglu, C., Sonmez, H.: Application of logistic regression for landslide susceptibility
691 zoning of Cekmece Area, Istanbul, Turkey. Environ. Geol, 51, 241–256, 2006.

692 Ermini, L, Catani, F., Casagli, N.: Artificial Neural Networks applied to landslide susceptibility assessment.
693 Geomorphology, 66, 327–343, 2005.

694 European Commission Humanitarian Aid, Civil Protection, U.N.I.S. for D.R.R.: Disaster Risk Reduction 20
695 Examples of Good Practice from Central Asia, 2006.

696 Frattini, P., Crosta, G., Carrara, A.: Techniques for evaluating the performance of landslide susceptibility models.
697 Engineering geology, 111(1-4), 62-72, 2010.

698 GFDRR (Global Facility for Disaster Reduction and Recovery): Disaster Risk Management Notes for Priority
699 Countries 2009-2015. Eur. Asia 48–49, 2009.

700 GFDRR (Global Facility for Disaster Reduction and Recovery): Europe and Central Asia-Country Risk Profiles
701 for Floods and Earthquakes. 144 pg, 2016.

702 Goetz, J.N., Brenning, A., Petschkoc, H. Leopold P.: Evaluating machine learning and statistical prediction tech-
703 niques for landslide susceptibility modeling. Comput Geosci., 81, 1-11, 2015.

704 Golovko, D., Roessner, S., Behling, R., Wetzel, H. U., Kleinschmidt, B: Development of multi-temporal landslide
705 inventory information system for southern Kyrgyz Republic using GIS and satellite remote sensing. PFG
706 2015, 157–172, 2015.

https://doi.org/10.5194/nhess-2023-33
Preprint. Discussion started: 28 February 2023

Havenith, H. B., Strom, A., Jongmans, D., Abdrakhmatov, A., Delvaux, D., Tréfois, P.: Seismic triggering of landslides, Part A: Field evidence from the Northern Tien Shan. Natural Hazards and Earth System Sciences, 3(1/2), 135-149, 2003.

Havenith, H.B., Strom, A., Cacerez, F., Pirard, E.: Analysis of landslide susceptibility in the Suusamyr region, Tien Shan: statistical and geotechnical approach. Landslides 3, 39–50, 2006a.

Havenith, H.B., Torgoev, I., Meleshko, A., Alioshin, Y., Torgoev, A., Danneels, G.: Landslides in the Mailuu-Suu Valley, Kyrgyz Republic—hazards and impacts. Landslides 3, 137–147, 2006b.

Havenith, H.B., Strom, A., Torgoev, I., Torgoev, A., Lamair, L., Ischuk, A., Abdrakhmatov, K.: Tien Shan geohazards database: Earthquakes and landslides. Geomorphology 249, 16–31, 2015a.

Havenith, H.B., Torgoev, A., Schlögel, R., Braun, A., Torgoev, I., Ischuk, A.: Tien Shan geohazards database: Landslide susceptibility analysis. Geomorphology 249, 32–43, 2015b.

Havenith, H.B., Torgoev, A., Braun, A., Schlögel, R., Micu, M.: A new classification of earthquake-induced landslide event sizes based on seismotectonic, topographic, climatic and geologic factors. Geoenvironmental Disasters, 1(3), 1-24, 2016.

Havenith, H.B., Umaraliev, R., Schlögel, R., Torgoev, I., Ruslan, U., Schlogel, R., Torgoev, I.: Past and Potential Future Socioeconomic Impacts of Environmental Hazards in Kyrgyz Republic. In Kyrgyz Republic: Political, Economic and Social Issues; Olivier, A.P., Ed.; Nova Science Publishers, Inc.: Hauppauge, NY, USA; pp. 63–113, 2017.

Hong, Y., Adler, R., Huffman, G.: Use of satellite remote sensing data in the mapping of global landslide susceptibility. Nat. Hazards, 43, 23–44, 2007.

Ishihara, K., Okusa, S., Oyagi, N., Ischuk, A.: Liquefaction-induced flow slide in the collapsible loess deposit in Soviet Tajik. Soils and foundations, 30(4), 73-89, 1990.

Juliev, M., Pulatov, A., Hubl, J.: Natural hazards in mountain regions of Uzbekistan: A review of mass movement processes in Tashkent province. International Journal of Scientific & Engineering Research, 8(2), 1102, 2017.

Kalmetieva, Z.A., Mikolaichuk, A. V, Moldobekov, B.D., Meleshko, A. V, Janaev, M.M., Zubovich, A. V.: Atlas of earthquakes in Kyrgyz Republic. Central-Asian Institute for Applied Geosciences and United Nations International Strategy for Disaster Reduction Secretariat Office in Central Asia, Bishkek, p 75, 2009.

Kirschbaum, D., Stanley, T., Zhou, Y.: Spatial and temporal analysis of a global landslide catalog. Geomorphology, 249, 4-15, 2015.

Lagomarsino, D., Tofani, V., Segoni, S., Catani, F., Casagli, N.: A tool for classification and regression using random forest methodology: Applications to landslide susceptibility mapping and soil thickness modeling. Environ. Model. Assess., 22, 201–214, 2017.

Lee, S.: Application of logistic regression model and its validation for landslide susceptibility mapping using GIS

https://doi.org/10.5194/nhess-2023-33
Preprint. Discussion started: 28 February 2023

and remote sensing data. Int. J. Remote Sens., 26, 1477–1491, 2005.

Li, F., Torgoev, I., Zaredinov, D., Li, M., Talipov, B., Belousova, A., Kunze, C., Schneider, P.: Influence of Earthquakes on Landslide Susceptibility in a Seismic Prone Catchment in Central Asia. Appl. Sci, 11, 3768, 2021.

Manzo, G., Tofani, V., Segoni, S., Battistini, A., Catani, F.: GIS techniques for regional-scale landslide susceptibility assessment: The Sicily (Italy) case study. Int. J. Geogr. Inf. Sci., 27, 1433–1452, 2013.

Martelloni, G., Segoni, S., Fanti, R., Catani, F.: Rainfall thresholds for the forecasting of landslide occurrence at regional scale. Landslides, 9, 485-495, 2012.

Medeu, A.R., Blagovechshenskiy, A.R.: Seismogenic Landslide risk zoning in the surrounding areas of Almaty city, Kazakhstan. Vestnick, 6, 121, 2016.

Molnar, P., Tapponnier, P.: Cenozoic Tectonics of Asia: Effects of a Continental Collision: Features of recent continental tectonics in Asia can be interpreted as results of the India-Eurasia collision. science, 189(4201), 419-426, 1975.

Nadim, F., Kjekstad, O., Peduzzi, P., Herold, C., Jaedicke, C.: Global landslide and avalanche hotspots. Landslides, 3(2), 159-173, 2006.

Niyazov, R.A.: Landslides in Uzbekistan. FAN, Tashkent, 207 pp (in Russian), 2009.

Niyazov, R.A., Nurtaev, B.S.: Evaluation of Landslides in Uzebekistan Caused by the Joint Impact of Precipitation and Deep-focus Pamir-Hindu Earthquakes. In Landslides: Global Risk Preparedness (pp. 253-265). Springer, Berlin, Heidelberg, 2013.

Niyazov R.A.: Uzbekistan landslides. Uzbekistan landslide service. Technical report, 2020a.

Niyazov, R., Nurtaev, B., Bimurzaev, G., Tashpulatov, M.: Flow Slides in Uzbekistan: Overview and Case Studies. In Workshop on World Landslide Forum (pp. 59-65). Springer, Cham, 2020b.

Pánek, T., Korup, O., Minár, J., Hradecký J.: Giant landslides and highstands of the Caspian Sea, Geology, 44 (11), 939–942, 2016.

Persits, F. M., Ulmishek, G. F., Steinshouer, D. W.: Maps showing geology, oil and gas fields and geologic provinces of the Former Soviet Union (No. 97-470-E). US Geological Survey, 1997.

Piroton, V., Schlögel, R., Barbier, C., Havenith, H.B.: Monitoring the recent activity of landslides in the Mailuu-suu valley (Kyrgyz Republic) using radar and optical remote sensing techniques. Geosciences, 10 (5), p. 164, 2020.

Pittore, M., Ozturk, U., Moldobekov, B., Saponaro, A.: EMCA Landslide catalog Central Asia. V. 1.0. GFZ Data Services, 2018.

Poggi, V. et al. a.: Harmonising seismicity information in Central Asia: earthquake catalogue and faults. The SFRARR probabilistic flood hazard assessment. In prep. for the Special Issue “Regionally consistent risk assessment for earthquakes and floods and selective landslide scenario analysis in Central Asia”. Natural

https://doi.org/10.5194/nhess-2023-33
Preprint. Discussion started: 28 February 2023

775 Hazards and Earth System Sciences (NHESS).

776 Poggi, V. et al. b.: Development of a state of art probabilistic seismic hazard model for Central Asia countries.
777 The SFRARR probabilistic flood hazard assessment. In prep. for the Special Issue “Regionally consistent
778 risk assessment for earthquakes and floods and selective landslide scenario analysis in Central Asia”. Natural
779 Hazards and Earth System Sciences (NHESS).

780 Pollner, J., Kryspin-Watson, J., Nieuwejaar, S.: Disaster Risk Management and Climate Change Adaptation in
781 Europe and Central Asia. World Bank 1–53, 2010.

782 Pusch, C.: A comprehensive risk management framework for Europe and Central Asia. (No. 9). Disaster Risk
783 Management Working Paper Series, 2004.

784 Reichenbach, P., Rossi, M., Malamud, B.D., Mihir, M., Guzzetti, F.: A review of statistically-based landslide
785 susceptibility models. Earth Sci. Rev. 180, 60–91, 2018.

786 Roessner, S., Wetzel, H. U., Kaufmann, H., Kornus, W., Lehner, M., Reinartz, P., Mueller, R. Landslide
787 Investigations in Southern Kyrgyz Republic Based on a Digital Elevation Model Derived from MOMS-2P
788 Data. IAPRS, Vol. 33, Part B7, Amsterdam, pp. 1259 -1266, 2000.

789 Roessner, S., Wetzel, H.U., Kaufmann, H., Sarnagoev, A.: Satellite Remote Sensing and GIS Based Analysis of
790 Large Landslides in Southern Kyrgyz Republic NATO Advanced Research Workshop: Security of Natural
791 and Artificial Rockslide Dams”, Bishkek, Kyrgyz Republic 2004.

792 Roessner, S., Wetzel, H.U., Kaufmann, H., Sarnagoev, A.: Potential of Satellite Remote Sensing and GIS for
793 Landslide Hazard Assessment in Southern Kyrgyz Republic (Central Asia)”, Natural Hazards, Vol. 35, No.
794 3, pp. 395 -416, 2005.

795 Saponaro, A., Pilz, M., Wieland, M., Bindi, D., Moldobekov, B., Parolai, S., Landslide susceptibility analysis in
796 data-scarce regions: the case of Kyrgyz Republic. Bull. Eng. Geol. Environ. 74, 1117–1136, 2014.

797 Scaini, C. et al.: (in prep.) A new regionally consistent exposure database for Central Asia: population and
798 residential buildings. In prep. for the Special Issue “Regionally consistent risk assessment for earthquakes
799 and floods and selective landslide scenario analysis in Central Asia”. Natural Hazards and Earth System
800 Sciences (NHESS).

801 Schiavina, M., Melchiorri, M., Pesaresi, M., Politis, P., Freire, S., Maffenini, L., Florio, P., Ehrlich, D., Goch, K.,
802 Tommasi, P., Kemper, T.: GHSL Data Package, Publications Office of the European Union, Luxembourg,
803 2022, ISBN 978-92-76-53071-8, JRC 129516, 2022.

804 Schlögel, R., Torgoev, I., De, Marneffe, C., Havenith, H.B.: Evidence of a changing size-frequency distribution
805 of landslides in the Kyrgyz Tien Shan, Central Asia. Earth Surf Process Landf 36(12), 1658– 1669, 2011.

806 Segoni, S., Tofani, V., Rosi, A., Catani, F. Casagli, N.: Combination of rainfall thresholds and susceptibility maps
807 for dynamic landslide hazardassessment at regional scale. Front Earth Sci., 6 (85), 2018.

808 Stanley, T., Kirschbaum, D.B.: A heuristic approach to global landslide susceptibility mapping. Nat. Hazards 87,

https://doi.org/10.5194/nhess-2023-33
Preprint. Discussion started: 28 February 2023

145–164, 2017.

Sternberg R.: Damming a river: a changing perspective on altering nature. Renewable Sustainable Energy Rev 10:165–197, 2006.

Strom, A.L., Korup, O.: Extremely large rockslides and rock avalanches in the Tien Shan, Kyrgyz Republic. Landslides 3, 125–136, 2006.

Strom, A.: Landslide dams in Central Asia region. Journal of the Japan Landslide Society, 47(6), 309-324, 2010.

Strom, A., Abdrakhmatov, K.: Large-Scale Rockslide Inventories: From the Kokomeren River Basin to the Entire Central Asia Region (WCoE 2014–2017, IPL-106-2, in: Workshop on World Landslide Forum. Springer, Cham, pp. 339–346, 2017.

Strom, A., Abdrakhmatov. K.: Rockslides and rock avalanches of Central Asia: distribution, morphology, and internal structure. Elsevier, 441pg. ISBN: 978-0-12-803204-6, 2018.

Styron, R., Pagani, M.: The GEM Global Active Faults Database." Earthquake Spectra, vol. 36, no. 1_suppl, Oct. 2020, pp. 160–180, 2020.

Tien Bui, D., Tuan, T. A., Klempe, H., Pradhan, B., Revhaug, I. Spatial prediction models for shallow landslide hazards: a comparative assessment of the efficacy of support vector machines, artificial neural networks, kernel logistic regression, and logistic model tree. Landslides, 13, 361-378, 2016.

Thurman, M.: Natural Disaster Risks in Central Asia: A Synthesis. UNDP BCPR, 2011.

Tiranti D., Nicolò G., Gaeta A. R.: Shallow landslides predisposing and triggering factors in developing a regional early warning system. Landslides 16 (2): 235–251, 2019.

Trifonov, V.G., Makarov, V.I., Scobelev, S.F.: The Talas-Fergana active right-slip faults. Ann Tectonicae 6:224–237, 1992.

Trigila, A., Frattini, P., Casagli, N., Catani, F., Crosta, G., Esposito, C., Spizzichino, D.: Landslide susceptibility mapping at national scale: the Italian case study, in: Landslide Science and Practice. Springer, Berlin, Heidelberg, pp. 287–295, 2013.

Ullah, S., Bindi, D., Pilz, M., Danciu, L., Weatherill, G., Zuccolo, E., . Anatoly Ischuk, A., Mikhailova, N.N., Abdrakhmatov, K., Parolai, S. Probabilistic seismic hazard assessment for Central Asia. Annals of Geophysics, 58(1), 2015.

UN ISDR.: Risk assessment for Central Asia and Caucasus: desk study review, CAC DRMI 2009, Risk Management Working Paper Series No. 9. The World Bank, 2009.

World Bank: Natural Disaster Hotspots: Case Studies. Disaster Risk Management Series No. 6, 2006.

World Bank: Investigation and Analysis of Natural Hazard Impacts on Linear Infrastructure in Southern Kyrgyz Republic Desk and Field Studies Report. Report 68669, 2008.

World Bank: The Global Landslide Hazard Map: Final Project Report. Appendix A., 2020.

https://doi.org/10.5194/nhess-2023-33
Preprint. Discussion started: 28 February 2023

842 Yaning, C.: Landslide-debris flow and its prevention in Kazakhstan. Arid Land Geography, 1992.

843 Yamazaki, D., Ikeshima, D., Tawatari, R., Yamaguchi, T., O'Loughlin, F., Neal, J. C., Sampson, C.C., Kanae, S.,
844 Bates, P.D.: A high-accuracy map of global terrain elevations. Geophysical Research Letters, 44(11), 5844-
845 5853, 2017.

846 Yilmaz, I.: Landslide susceptibility mapping using frequency ratio, logistic regression, artificial neural networks
847 and their comparison: a case study from Kat landslides (Tokat—Turkey). Computers & Geosciences, 35 (6):
848 1125-1138, 2009.

849 Zubovich, A. V., Wang, X. Q., Scherba, Y. G., Schelochkov, G. G., Reilinger, R., Reigber, C., Mosienko, O.,
850 Molnar, P., Michajljow, W., Makarov, V.I., Li, J., Kuzikov, S.I., Herring, T.A., Hamburger, M.W., Hager
851 B.H., Dang, Y., Bragin, V.D., Beisenbaev, R.: GPS velocity field for the Tien Shan and surrounding regions.
852 Tectonics, 29(6), 2010.

853